Am J Cancer Res 2024;14(1):300-323
www.ajcr.us /ISSN:2156-6976/ajcr0154637

Original Article

Experimental treatment efficacy of dmrFABP5 on prostate cancer singly or in combination with drugs in use

Saud A Abdulsamad[1,2], Abdulghani A Naeem[1,2], Hao Zeng[1], Gang He[2,3], Xi Jin[1], Bandar A Alenezi[2], Jianzhong Ai[1], Jiacheng Zhang[2], Hongwen Ma[1], Philip S Rudland[4], Youqiang Ke[1,2,3]

[1]Institute of Urology, West China Hospital, Sichuan University, No. 37 Guo Xue Xiang, Chengdu 610041, Sichuan, China; [2]Department of Molecular and Clinical Cancer Medicine, Liverpool University, CRC Building, No. 200 London Road, Liverpool L3 9TA, UK; [3]Sichuan Industrial Institute of Antibiotics, Chengdu University, Chengdu 610081, Sichuan, China; [4]Department of Biochemistry and Systems Biology, Bioscience Building, Crown Street, Liverpool L69 3BX, UK

Received November 27, 2023; Accepted January 12, 2024; Epub January 15, 2024; Published January 30, 2024

Abstract: Enzalutamide is a drug used to treat prostate cancer (PC) and docetaxel is a drug for chemotherapeutic treatment of diverse cancer types, including PC. The effectiveness of these drugs in treating castration-resistant prostate cancer (CRPC) is poor and therefore CRPC is still largely incurable. However, the bio-inhibitor of fatty acid-binding protein 5 (FABP5), dmrFABP5, which is a mutant form of FABP5 incapable of binding to fatty acids, has been shown recently to be able to suppress the tumorigenicity and metastasis of cultured CRPC cells. The present study investigated the possible synergistic effect of dmrFABP5 combined with either enzalutamide or docetaxel on suppressing the tumorigenic properties of PC cells, including cell viability, migration, invasion and colony proliferation in soft agar. A highly significant synergistic inhibitory effect on these properties was observed when dmrFABP5 was used in combination with enzalutamide on androgen-responsive PC 22RV1 cells. Moreover, a highly significant synergistic inhibitory effect was also observed when dmrFABP5 was combined with docetaxel, and added to 22RV1 cells and to the highly malignant, androgen-receptor (AR)-negative Du145 cells. DmrFABP5 alone failed to produce any suppressive effect when added to the FABP5-negative cell line LNCaP, although enzalutamide could significantly suppress LNCaP cells when used as a single agent. These synergistic inhibitory effects of dmrFABP5 were produced by interrupting the FABP5-related signal transduction pathway in PC cells. Thus, dmrFABP5 appears to be not only a potential single therapeutic agent, but it may also be used in combination with existing drugs to suppress both AR-positive and AR-negative PC.

Keywords: DmrFABP5, prostate cancer, CRPC, enzalutamide, docetaxel, synergistic effect

Introduction

Despite the improvements in chemotherapeutic and anti-androgen therapies in recent years, prostate cancer (PC) remains the second most common cause of cancer-related mortalities in men in developed countries [1]. PC responds well to anti-androgen treatments at an early stage, but in the majority of cases, the cancer relapses and becomes castration-resistant in ~2 years after the initial treatment. The growth and dissemination of castration-resistant prostate cancer (CRPC) no longer relies on male androgen stimulation, and CRPC responds poorly to further androgen deprivation therapy (ADT). Therefore, CRPC currently remains an incurable disease. Thus, it is imperative to understand the molecular mechanisms involved in the conversion of cancer cells from an androgen-dependent to an androgen-independent state, so that new strategies may be identified to treat this aggressive CRPC [2]. Like the majority of adenocarcinomas, cancer of the prostate needs lipids as an energy source to fuel its development and expansion; thus, dysregulated lipid metabolism is well known to be associated with the onset and progression of PC cells [3-6]. In addition, the lipid-degraded products, namely fatty acids, participate in a variety of biological processes by acting as key

signalling molecules in pathways involved in the advancement of PC. One such related molecule is fatty acid-binding protein 5 (FABP5) [7, 8]. It is a member of a family of intracellular lipid chaperones that transport fatty acids to their nuclear receptor peroxisome proliferator-activated receptor (PPARγ). This interaction results in the upregulation of the pro-angiogenic protein vascular endothelial growth factor (VEGF), which, in turns, can lead to the malignant progression of CRPC cells [9-12]. In normal prostate cells, FABP5 is either not expressed or expressed at a markedly low level, but its expression is greatly increased in PC cells. The increased level of FABP5 in prostate carcinomas significantly correlates with the degree of malignancy measured by combined Gleason scores. The highest level of FABP5 is expressed by the most advanced, highly malignant carcinoma types [8-10, 12]. Moreover, the nuclear fatty acid receptor PPARγ, which upregulates the expression of the *VEGF* gene, is greatly increased when responding to fatty acid stimulation, and this increase is significantly associated with reduced patient survival times [8-10].

Since increased expression of FABP5 is a strong factor in promoting the malignant progression of PC cells [9, 10, 13], targeting this increased FABP5 may be a novel strategy to suppress the malignant progression of cancer cells [14]. Recently, a chemical inhibitor of FABP5, named SB-FI-26, originally developed as an anti-inflammatory and anti-nociceptive drug [15], was used to treat CRPC cells. It produced a 9-fold suppression of the primary tumour mass and a 50% suppression of tumour metastasis in an experimental nude mouse model [16]. More recently, a potent FABP5 bioinhibitor called dmrFABP5 has been developed, which is a recombinant protein with 2 of the 3 key amino acids in the fatty acid-binding motif of FABP5 mutated. When tested in a nude mouse model, dmrFABP5 produced a 14-fold reduction in the primary tumour mass and a 100% suppression of tumour metastasis [17]. Moreover, SB-FI-26 competitively inhibited the cellular uptake of fatty acids and disrupted the FABP5-PPARγ-VEGF signalling transduction pathway in CRPC cells. However, the molecular mechanisms by which dmrFABP5 suppresses cancer cell proliferation are not fully understood, and recent evidence suggests that dmrFABP5 may be involved in promoting the apoptosis of cancer cells by reversing the biological function of FABP5 [17-19].

There are a number of standard chemotherapeutic agents for CRPC treatment such as docetaxel [20, 21], which targets microtubules, disrupts the cell cycle and promotes apoptosis [22]. Docetaxel plays a significant role in the increased level of acetylation of α-tubulins, which can lead to a reduction in the VEGF level, an increase in apoptosis [23, 24], and a downregulation of androgen receptor (AR) [25]. Moreover, docetaxel can suppress *Bcl-2* expression and increase the level of Bax proteins, thereby disrupting the balance between promoting and suppressing apoptosis [26, 27]. Although docetaxel is often used for clinical treatment, resistance to this drug frequently develops in PC cells [28]. Regarding ADT, the AR inhibitor enzalutamide is a novel anti-androgen that has been used to treat CRPC [29, 30], but resistance to this treatment still develops [31-33]. Resistance to enzalutamide is considered to be related to the generation of AR spliced variants, particularly AR-V7 [34-37], which lacks the ligand-binding domain (LBD). Therefore, it has been reported that enzalutamide is not able to bind to AR-V7, and thus the treatment effect is poor in such cases [38].

Treatment of PC with docetaxel and enzalutamide suppresses tumorigenicity of the cancer cells by targeting different mechanisms, but the development of resistance to both separate treatments appears to be inevitable [20, 21, 31, 39]. At present, it is not clear whether combination therapy can improve antitumor activity or reduce resistance to docetaxel and enzalutamide, perhaps by minimising the side effects associated with chemotherapy and ADT [40-42]. The current study aims to investigate the complex association between different doses and combinations of dmrFABP5 and either docetaxel or enzalutamide for suppressing the malignant progression of CRPC cells.

Materials and methods

Cell lines and culture

Various well-characterised PC cell lines are widely used for testing new drugs [43]. Thus, the present study used the following 3 cell lines

(ATCC, USA): Du145, 22RV1 and LNCaP. Du145 is a highly malignant PC cell line established from a brain metastasis. Du145 does not express AR but expresses high levels of FABP5 [7, 8]. 22RV1 is a moderately malignant cell line established from an original prostate carcinoma. This cell line expresses moderately high levels of both AR and FABP5. LNCaP is a weakly malignant cell line established from a lymph node adjacent to an original carcinoma. It does not express FABP5, but it can express AR [44]. All cell lines were cultured in complete medium containing RPMI 1640 (Gibco; Thermo Fisher Scientific, Inc.) supplemented with 5 ml L-glutamine (20 mM), 10% (v/v) FBS (Gibco; Thermo Fisher Scientific, Inc.) and 100 U/ml penicillin/streptomycin (Sigma-Aldrich; Merck KGaA), and incubated in a 37°C incubator with a humid atmosphere of 5% (v/v) CO_2, 95% (v/v) air. The culture medium was replaced every 3 days and cells proliferated as monolayers. The cultured cells were subjected to short tandem repeats profile analysis every 3 years to ensure their authenticity.

Expression of dmrFABP5 in Escherichia coli (E. coli) cells

The process employed to produce recombinant dmrFABP5 was similar to that reported previously [17]. The DNA plasmid (BD Biosciences CloneTech, CA, USA) containing the expression construct was transformed into the DH5α strain of *E. coli* cells. A single colony harbouring the expression construct was picked up with a sterile loop from a selective antibiotic (ampicillin)-containing Luria-Bertani (LB) agar plate, inoculated into 10 ml LB medium with 50 μg/ml ampicillin in a 50-ml flask, and incubated overnight at 37°C with 230 rpm agitation. The overnight bacterial culture (10 ml) was transferred into a flask with 250 ml prewarmed medium and ampicillin, and cultured at 37°C with constant agitation until the optical density at 600 nm reached 0.6. Next, isopropylthiogalactoside (IPTG) (Sigma-Aldrich; Merck KGaA) was added to a final concentration of 1 mM to stimulate the expression of the recombinant protein. The largest quantity of recombinant protein was produced during the first 4 h after IPTG induction. The culture was then centrifuged at 4,000×g for 30 min to collect the cells, and the pellets were kept at -20°C in a freezer (Bako, UK) until subsequent experiments.

DmrFABP5 protein purification

N-Terminus pQE 30 series vectors (Qiagen, Inc.) were used to express a high level of N-terminally 6× His-tagged recombinant FABP5 in DH5α *E. coli* cells. 6-His-tagged proteins were purified using a Ni-NTA Fast Start Kit (Qiagen, Inc.). Bacterial cell pellets were suspended in 10 ml Lysis Buffer (pH 8.0), incubated at room temperature for 60 min, and then centrifuged at 14,000×g for 30 min at 4°C. The recombinant protein-containing supernatant was extracted from the debris, collected and placed onto a Ni-NTA column (included in the kit, Qiagen, Inc.) that was conjugated to an anti-6-His-tag antibody. The recombinant protein attached to the anti-6-His-tag antibody was eluted after three washes with 4 ml Washing Buffer (pH 8.0). As previously described [17], the two eluted fractions were collected, and samples were subjected to SDS-PAGE and Western blot as instructed by the manufacturer to establish the size and purity of the resultant recombinant protein (data not shown).

Drug preparation and treatment plans

Docetaxel and enzalutamide, which were purchased from MedChem Express, were dissolved in dimethyl sulfoxide (DMSO) to prepare a stock solution. To avoid repeated freezing, drugs were diluted in DMSO, aliquoted and stored at -80°C. Cells were first treated with each single agent at different dilutions to identify the concentration that inhibited cell proliferation by 50% (that is the IC_{50}). The combination treatment groups for the *in vitro* assays were evaluated by using the concentrations corresponding to the IC_{50} of every single agent.

Cell viability and combination index (CI) assays

Du145 cells were plated at 5,000 cells/well, whilst 22RV1 and LNCaP cells were plated at 10,000 cells/well in a 96-well plate and treated with each drug alone, to evaluate cell viability and determine the IC_{50}. Controls were treated with DMSO for docetaxel and enzalutamide experiments, and with PBS for dmrFABP5 experiments. For Du145 and 22RV1 cells, dmrFABP5 was used from 0.05-20 μM concentrations, while docetaxel was used at doses ranging from 0.001 to 200 nM and enzalutamide from 1-100 μM. For LNCaP cells, the

concentrations used ranged from 0.001-100 μM.

Cells were incubated with each drug either singly or in combination with dmrFABP5 using different concentrations for 72 h. Cells were then evaluated with PrestoBlue HS viability reagent (Invitrogen; Thermo Fisher Scientific, Inc.), and the results of cell viability were calculated as a percentage of the control. The mean ± SEM of 3 separate experiments are shown. Synergistic interactions were evaluated according to the Chou-Talalay method by using CompuSyn to calculate the CI. Values <0.9 were considered to be synergistic [45].

Invasion assays

The invasive abilities of the cells were assessed using Boyden Chambers in a 24-well plate containing 8-μM pore membranes. Du145, 22RV1 and LNCaP cells were seeded in the upper compartment with 0.1% (v/v) DMSO for the control group. Du145 and 22RV1 cells were treated for 24 h with dmrFABP5 at doses of 5, 10 and 20 μM; docetaxel at doses of 2.5, 3 and 4 nM; and enzalutamide at doses of 10 and 100 μM. For LNCaP cells, the dmrFABP5 dose was selected as 100 nM alone or in combination with either drug. In the lower compartment of each Boyden Chamber, 500 μl complete RPMI 1640 medium was added as a chemoattractant, while in the upper compartment, 500 μl serum-free RPMI 1640 medium supplemented with 100 U penicillin/streptomycin was added. Cells with invasive abilities were able to invade through the Matrigel (supplied with the chamber) via the pores. The invaded cells were stained with crystal violet and counted. The mean ± SEM of 3 separate experiments are shown.

Wound healing assay

Ibidi culture insets in an μ-dish were used to assess the migration and wound closure abilities of cells. The combination treatment time points were evaluated according to the aggressiveness of the cells. Thus, Du145 was evaluated at 0, 12 and 24 h, whilst 22RV1 and LNCaP cells were evaluated at 0, 24, 48 and 72 h. The combination treatment methods used in the present study have been described previously [46]. The mean percentage of the original width of the wound ± is shown for 3 separate experiments.

Colony formation assay in soft agar

The soft agar assay, a method for testing the anchorage-independent proliferation of the cells, was carried out in 6-well plates that had been pre-coated with 2 ml 1% (w/v) low melting agarose in complete culture medium and hardened for 10 min in a 4°C refrigerator. Du145, 22RV1 and LNCaP cells were cultured to 60-80% confluence in a flask, collected and then suspended in RPMI complete culture medium. The cells were plated in triplicate into 0.5% (v/v) agar in 6-well plates with complete culture medium on the top layer of the well, and the plates were placed in the refrigerator for 10 min until the agar hardened. Du145, 22RV1 and LNCaP cells were seeded at 60,000 cells per well in 6-well plates and incubated at 37°C in an atmosphere of 5% (v/v) CO_2, 95% (v/v) air. After 1 week of incubation, 250 μl medium alone or medium containing a single agent or a combination of agents was added to the 6-well plates. After 3 weeks, the 6-well plates were treated with 0.5 mg/ml MTT at a concentration of 0.5 mg/ml for 4 h at 37°C. The number of colonies growing in suspension was counted with GelCount (Oxford Optronix). Colonies were only counted if their diameter was ≥250 μm for Du145 and 22RV1 cells, and ≥150 μm for LNCaP cells. The mean ± SEM of 3 separate experiments are shown.

Western blotting

Cells were washed twice with PBS and lysed with lysis buffer containing protease inhibitors (Qiagen, Inc.). Cell lysates were centrifuged at 4000 g for 15 min at 4°C, and the supernatant collected and the protein concentration was estimated by Bradford assay (Quick Start Bradford Protein Assay; Bio-Rad Laboratories, Inc.). Proteins (20 μg per sample) were loaded on a Mini protein gel (Bio-Rad Laboratories, Inc.) containing 15% (w/v) polyacrylamide, and, after electrophoresis, they were transferred to PVDF membranes (MilliporeSigma). The membranes were incubated in blocking buffer [5% (v/v) TBS-Tween 20 (TBS-T) in 0.1% (w/v) skimmed milk] for 1 h, and then washed three times with TBS-T for 15 min. Next, the membranes were incubated with primary antibodies against AR (1:400 dilution), VEGF (1:1,000), PPARγ (1:200), phosphorylated (p)-PPARγ (1:500), Sp1 (1:1,000), Bcl-2 (1:500), Bax

Table 1A. Antibodies used in detection of recombinant FABP5

Protein	Primary Antibody	Secondary Antibody
FABP5	Rabit Antihuman Monoclonal (1:500) (HycultR Biotech)	Swine Anti-Rabit Polyclonal HRP (1:10,000) (DAKO)
6-His-tagged	Penta-His Mouse Monoclonal (1:1000) (Qiagen)	Rabit-Anti-Mouse Polyclonal HRP (1:10,000) (DAKO)
β-Actin	Mouse Monoclonal Anti-β-Actin (1:20,000) (Abcam)	Rabit-Anti-Mouse Polyclonal HRP (1:20,000) (DAKO)

Table 1B. Antibodies and dilutions used for detection of different proteins

AR	Mouse monoclonal (1:400) (Santa Cruz)	Rabbit Anti-Mouse Polyclonal HRP (1:10,000) (DAKO)
AR-V7	Rabbit polyclonal (1:1000) (Cell Signalling)	Swine Anti-Rabbit Polyclonal HRP (1:10,000) (DAKO)
Sp1	Rabbit polyclonal (1:1000) (Cell Signalling)	Swine Anti-Rabbit Polyclonal HRP (1:10,000) (DAKO)
Bcl-2	Mouse monoclonal (1:250) (Santa Cruz)	Rabbit Anti-Mouse Polyclonal HRP (1:10,000) (DAKO)
BAX	Mouse monoclonal (1:500) (Santa Cruz)	Rabbit Anti-Mouse Polyclonal HRP (1:10,000) (DAKO)
PPARγ	Mouse monoclonal (1:500) (Santa Cruz)	Rabbit Anti-Mouse Polyclonal HRP (1:10,000) (DAKO)
pPPARγ (Ser112)	Rabbit polyclonal phospho-PPARγ (Ser112) (1:250) (Thermo Fisher)	Swine Anti-Rabbit Polyclonal HRP (1:10,000) (DAKO)
VEGF	Rabbit polyclonal (1:1000) (Abcam)	Swine Anti-Rabbit Polyclonal HRP (1:10,000) (DAKO)

(1:500), acetylated α-tubulin (1:300) and β-actin (1:5,000) (for normalization) overnight at 4°C. Membranes were then washed three times with T-BST for 15 min, and incubated with the secondary antibodies polyclonal rabbit anti-mouse IgG-horseradish peroxidase (HRP) (1:10,000) or polyclonal swan anti-rabbit IgG-HRP (1:10,000) for 2 h at room temperature. The detailed antibodies used in FABP5 detection are shown in **Table 1A**. Antibodies used for detection of other protein are shown in **Table 1B**. The bands on the membranes were then visualized with Immobilon ECL Ultra Western HRP Substrate (cat no. #WBULS0500; Merck KGaA) using a ChemiDoc imaging system (Bio-Rad). The bands on the blot were quantified with ImageJ 1.48 software. Results are expressed as a mean (± SEM) percentage normalised to that for β-actin from 3 different experiments.

Statistical analysis

Each experiment was conducted in triplicate and data are presented as the mean ± standard error (SEM). Student's t-test was used to compare means (paired) using GraphPad Prism 9 (GraphPad Software; Dotmatics). $P<0.05$ was considered to indicate a statistically significant difference. The control was compared with each single agent treatment and each single agent treatment was compared with the combination treatment. Synergistic interaction was evaluated according to the Chou-Talalay method using CompuSyn software to calculate CI. CI values <0.9 were considered to be synergistic [45].

Results

Compound concentrations used to achieve 50% proliferation inhibition of PC cells

Different concentrations of the above three compounds were added to the PC cell lines, and cell viability was recorded at 72 h as a percentage of the control (**Figure 1**). The IC_{50} concentrations of docetaxel in Du145, 22RV1 and LNCaP cells were 3, 4 and 2.2 nM, respectively (**Figure 1A-C**). Since enzalutamide failed to achieve significant inhibition of Du145 and 22RV1 cells (**Figure 1D** and **1E**), no IC_{50} could be calculated. In LNCaP cells, the IC_{50} concentration of enzalutamide was 97 nM (**Figure 1F**). The IC_{50} concentration of dmrFABP5 in Du145 and 22RV1 cells was 5 and 12 μM, respectively (**Figure 1G** and **1H**). Since dmrFABP5 did not cause inhibition of FABP5-negative LNCaP cells (**Figure 1I**), its IC_{50} in this cell line could not be calculated.

Effect of dmrFABP5 in combination with docetaxel in PC cell lines

The effect of dmrFABP5 combined with docetaxel on Du145 cells is shown in **Figure 2**, and the results of CI analysis results are shown in **Table 2**. When a fixed concentration of dmrFABP5 (5 μM) was combined with docetaxel at different concentrations (3, 0.3 and 0.03 nM) in Du145 cells, it suppressed cell proliferation by 89, 66 and 58%, respectively, compared to 51, 46 and 29%, respectively for docetaxel alone (**Figure 2A**). This yielded CIs of 0.00714, 0.38970 and 0.6585, respectively (**Table 2A**).

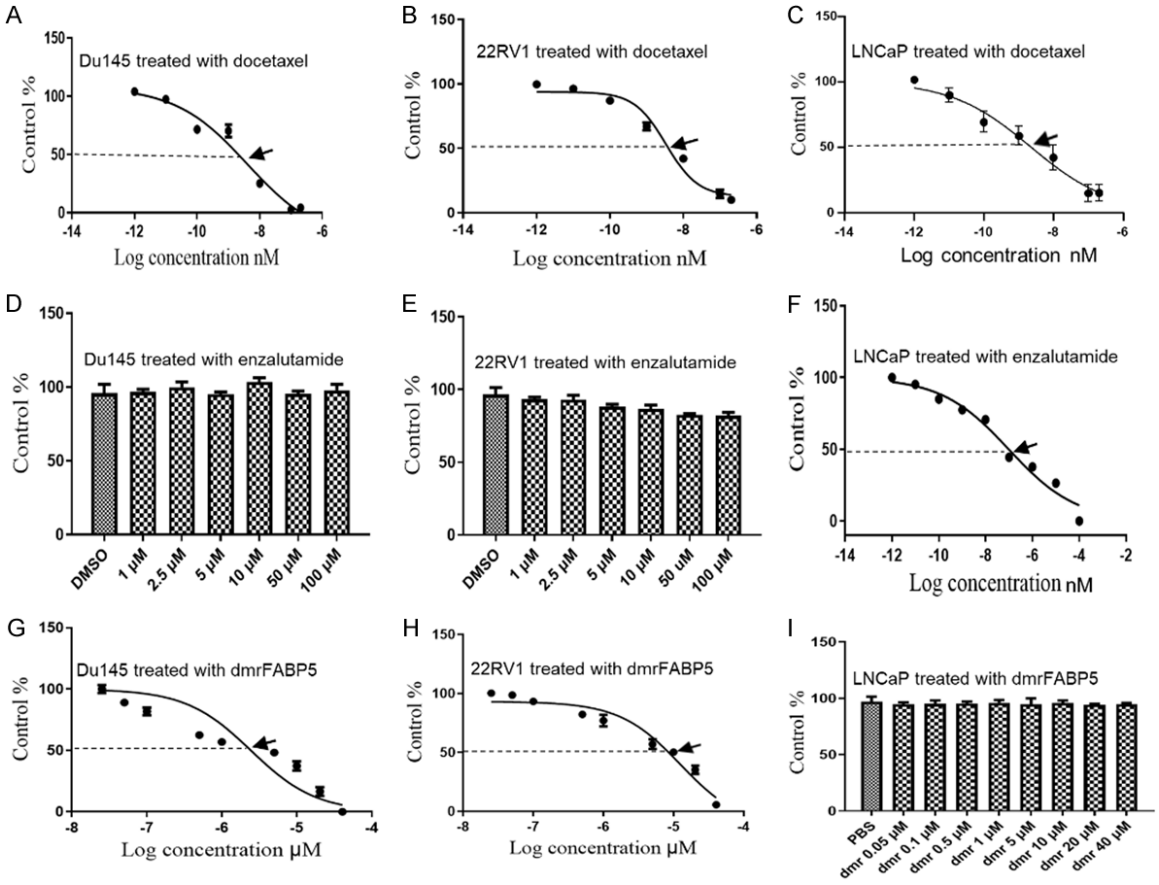

Figure 1. Determination of IC_{50} values for viability of cells treated with different concentrations of each compound. The cell viability of the prostate cancer cell lines (A) Du145, (B) 22RV1 and (C) LNCaP was evaluated upon treatment with different concentrations of docetaxel. The viability of (D) Du145, (E) 22RV1 and (F) LNCaP cells was determined treatment with different concentrations of enzalutamide. The viability of (G) Du145, (H) 22RV1 and (I) LNCaP cells was determined upon treatment with different concentrations of dmrFABP5. IC_{50} values were calculated for each cell line as described in the Materials and methods section, and are depicted by an arrowhead. IC_{50}, half-maximal inhibitory concentration.

No synergistic interaction for the combination of dmrFABP5 with docetaxel at 0.003 nM was observed. Similar synergistic effects were found when a fixed concentration of docetaxel (3 nM) was combined with dmrFABP5 at different concentrations (5, 1 and 0.5 μM), producing inhibitions of 86, 60 and 48% respectively, compared to 52, 38 and 30%, respectively, for dmrFABP5 alone (**Figure 2B**). This result yielded CI values of 0.00445, 0.1639 and 0.2281, respectively. No synergistic enhancement was found when 3 nM docetaxel was combined with 0.1 μM dmrFABP5 (**Table 2B**).

Further synergistic interactions were obtained in 22RV1 cells when a fixed dose of dmrFABP5 (10 μM) was added to 4, 0.4, 0.04 and 0.004 nM docetaxel (**Figure 3** and **Table 3**). It yielded reductions of 92, 78, 53 and 52%, respectively (**Figure 3A**), and CI values of 0.06834, 0.61895, 0.81263 and 0.71955, respectively (**Table 3A**). Similarly, when a fixed dose of docetaxel (4 nM) was combined with dmrFABP5 at 10, 5 and 1 μM, it yielded reductions of 93, 69 and 67%, respectively compared with reductions of 53, 49 and 36%, respectively for dmrFABP5 alone (**Figure 3B**). These suppressions were synergistic interactions with CI values of 0.07239, 0.53598 and 0.38839, respectively (**Table 3B**). The maximum suppression was found when the two compounds were added together at their IC_{50} (CI=0.06834). There was no synergistic effect when dmrFABP5 at 0.5 μM was added alongside 4 nM docetaxel (CI=7.43467) (**Table 3B**).

Both compounds were used to treat LNCaP cells, but no synergistic interactions were

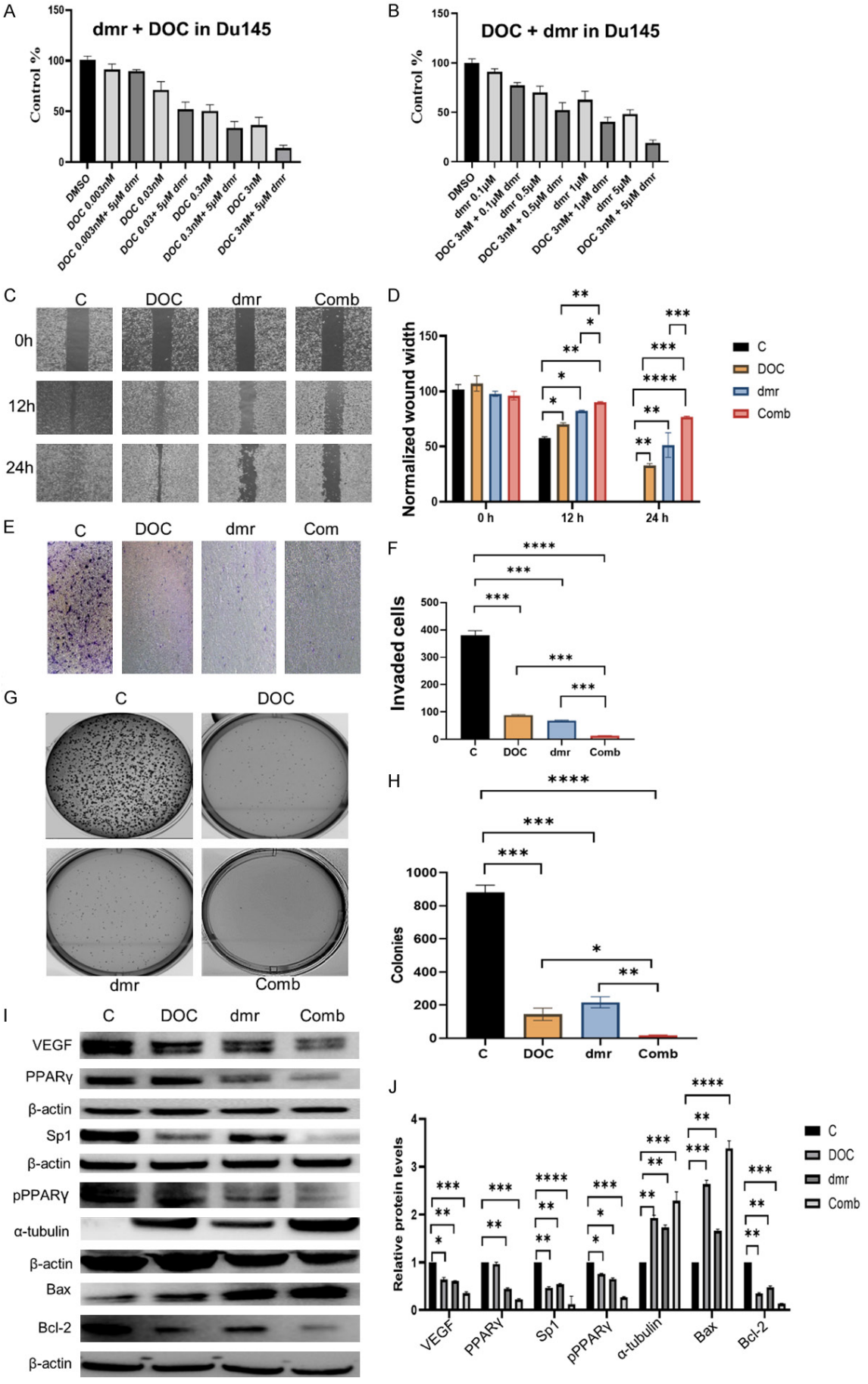
A
dmr + DOC in Du145
Control %
DMSO
DOC 0.003nM
DOC 0.003nM+ 5μM dmr
DOC 0.03nM
DOC 0.03+ 5μM dmr
DOC 0.3nM
DOC 0.3nM+ 5μM dmr
DOC 3nM
DOC 3nM+ 5μM dmr
B
DOC + dmr in Du145
Control %
DMSO
dmr 0.1μM
DOC 3nM + 0.1μM dmr
dmr 0.5μM
DOC 3nM + 0.5μM dmr
dmr 1μM
DOC 3nM+ 1μM dmr
dmr 5μM
DOC 3nM + 5μM dmr
C
C
DOC
dmr
Comb
0h
12h
24h
D
Normalized wound width
0 h
12 h
24 h
C
DOC
dmr
Comb
E
C
DOC
dmr
Com
F
Invaded cells
C
DOC
dmr
Comb
G
C
DOC
dmr
Comb
H
Colonies
C
DOC
dmr
Comb
I
C
DOC
dmr
Comb
VEGF
PPARγ
β-actin
Sp1
β-actin
pPPARγ
α-tubulin
β-actin
Bax
Bcl-2
β-actin
J
Relative protein levels
VEGF
PPARγ
Sp1
pPPARγ
α-tubulin
Bax
Bcl-2
C
DOC
dmr
Comb

Figure 2. Effect of dmrFABP5 on the tumor-suppression activity of docetaxel and relevant regulators in Du145 cells. A. Effect on the viability (as a percentage of the control) of cells treated with a fixed dose of dmrFABP5 combined with different doses of docetaxel for 72 h. B. Effect on the viability (as a percentage of the control) of cells treated with a fixed dose of docetaxel combined with different doses of dmrFABP5 for 72 h. C. Effect of dmrFABP5 combined with docetaxel on cell migration in wound healing at 24 h. Magnification: 20×. D. Quantitative assessment of the width of the remaining wound expressed as a percentage of that of the original wound. E. Effect of dmrFABP5 combined with docetaxel on cell invasion at 24 h. Magnification: 40×. F. Quantitative assessment of the numbers of invaded cells at 24 h. G. Effect of dmrFABP5 combined with docetaxel on cell anchorage-independent proliferation in soft agar. Colonies >250 μm in diameters were counted. H. Quantitative assessment of the number of colonies formed in soft agar after 21 days. I. Western blotting analysis of the effect of dmrFABP5 combined with docetaxel on the levels of protein regulators after 24 h of treatment. J. Quantitative assessment of the results of Western blotting for vascular endothelial growth factor, PPARγ, phosphorylated PPARγ, Bax, and Bcl-2, normalized first to β-actin and then to the control. Each experiment was performed in triplicate and the data are presented as the mean ± standard error of the mean. Student's t-test was used to compare the means. $P<0.05$ was considered to indicate a statistically significant difference. $^{*}P<0.05$, $^{**}P<0.001$, $^{***}P<0.0001$, $^{****}P<0.00001$. C, control; dmr, dmrFABP5; DOC, docetaxel; Com, combination of dmr and DOC; FABP5, fatty acid-binding protein 5; PPARγ, peroxisome proliferator-activated receptor.

Table 2. Combination Index (CI) analysis for dmrFABP5 combined with docetaxel in Du-145 cells

A. Fixed concentration of dmrFABP5 combined with different concentrations of docetaxel					
Cell lines	Dmr, μM	Docetaxel, nM	Suppression %	CI values	Relationship
Du145	5	3	86	0.007	Synergistic
Du145	5	0.3	67	0.389	Synergistic
Du145	5	0.03	48	0.658	Synergistic
Du145	5	0.003	12	12.176	Not synergistic
B. Fixed concentration of docetaxel combined with different concentrations of dmrFABP5					
Cell lines	Dmr, μM	Docetaxel, nM	Suppression %	CI values	Relationship
Du145	0.1	3	23	2.4818	Not synergistic
Du145	0.5	3	48	0.2281	Synergistic
Du145	1	3	60	0.1639	Synergistic
Du145	5	3	81	0.0044	Synergistic

observed (**Figure 4**). Thus, when a fixed dose of dmrFABP5 at 20 μM was mixed with docetaxel at 20, 2, 0.2 and 0.02 nM (**Figure 4A**), they produced inhibitions of 61, 47, 32 and 15%, respectively, compared to 63, 51, 33 and 14%, respectively, for docetaxel alone. Similarly, when a fixed dose of docetaxel at 2 nM was combined with dmrFABP5 at 20, 10, 5 and 1 μM (**Figure 4B**), it was suppressed by 45, 42, 44 and 47%, respectively, compared to 6, 5, 3 and 5% suppression, respectively, for dmrFABP5 alone. This yielded CIs>1.000.

Effect of dmrFABP5 in combination with enzalutamide on PC cell lines

The combination of dmrFABP5 with enzalutamide (**Figure 5**) did not produce any synergistic effect, although dmrFABP5 alone significantly suppressed Du145 cell proliferation. When dmrFABP5 was fixed at 5 μM and added alongside enzalutamide at 100, 50, 10 and 1 μM, this inhibited cell proliferation by 51, 43, 45 and 47%, respectively, compared to inhibitions of 4, 6, 5 and 1%, respectively, caused by enzalutamide alone (**Figure 5A**). This yielded CIs>1.000. A similar lack of synergistic effect was observed when a fixed dose of enzalutamide at 100 μM was added alongside 5, 1, 0.5 and 0.1 μM dmrFABP5 (**Figure 5B**). This suppressed proliferation by 47, 44, 29 and 8%, respectively. By contrast, dmrFABP5 alone produced 51, 47, 31 and 9% inhibition, respectively. This yielded CIs>1.000.

By contrast, a synergistic effect was achieved when dmrFABP5 was combined with enzalutamide on 22RV1 cells (**Figure 6** and **Table 4**). Thus, when a fixed dose of dmrFABP5 at 10 μM was added with enzalutamide at 50, 10 and 5 μM (**Figure 6A**), it produced suppressions of 87, 77 and 45%, respectively, compared to enzalutamide alone at 16, 11 and 7%, respectively. This yielded CIs of 0.14490, 0.10838 (as a

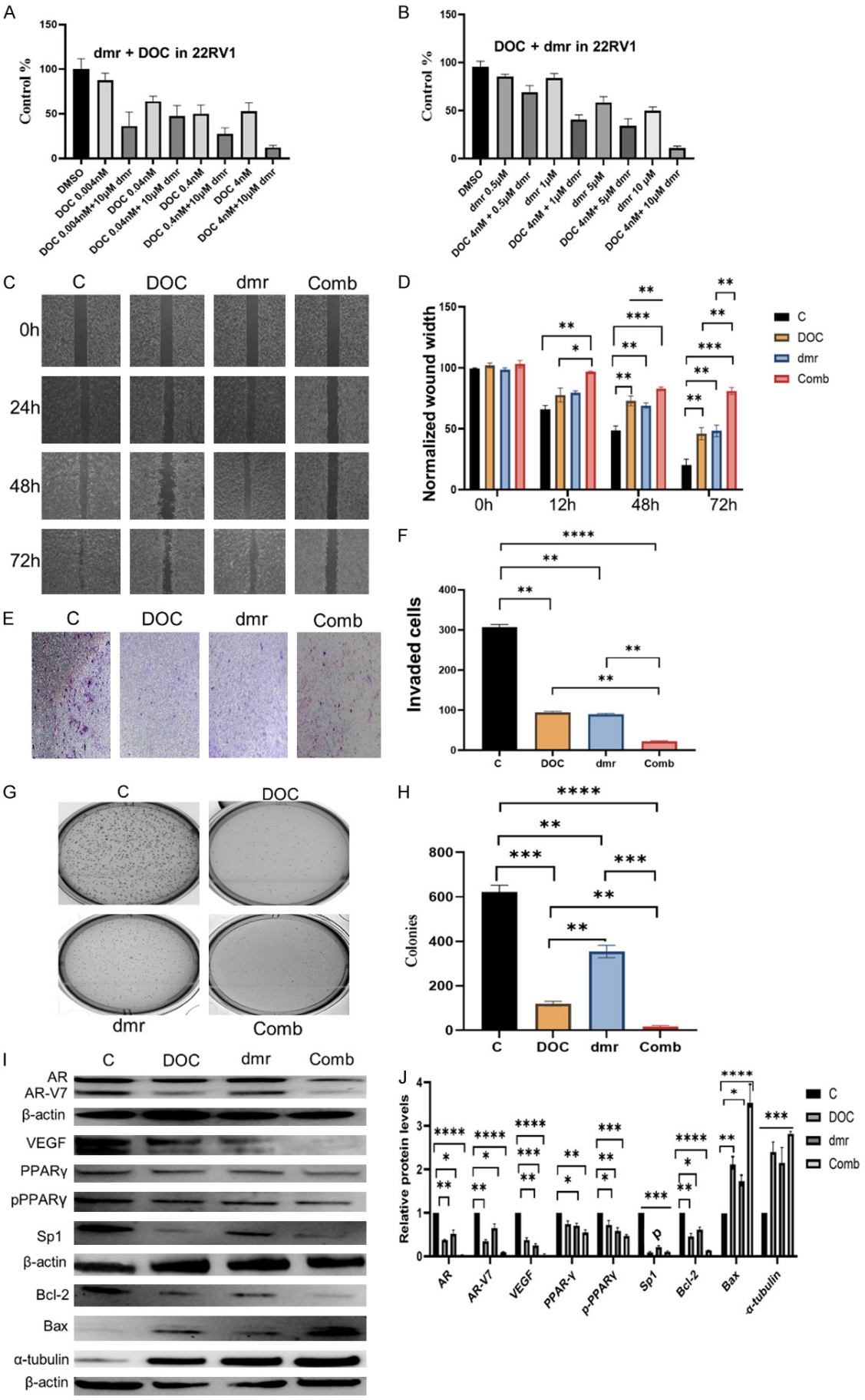
A
dmr + DOC in 22RV1
Control %
DMSO
DOC 0.004nM
DOC 0.004nM+10μM dmr
DOC 0.04nM
DOC 0.04nM+ 10μM dmr
DOC 0.4nM
DOC 0.4nM+10μM dmr
DOC 4nM
DOC 4nM+10μM dmr
B
DOC + dmr in 22RV1
Control %
DMSO
dmr 0.5μM
DOC 4nM + 0.5μM dmr
dmr 1μM
DOC 4nM + 1μM dmr
dmr 5μM
DOC 4nM+ 5μM dmr
dmr 10 μM
DOC 4nM+ 10μM dmr
C
C
DOC
dmr
Comb
0h
24h
48h
72h
D
Normalized wound width
0h
12h
48h
72h
C
DOC
dmr
Comb
E
C
DOC
dmr
Comb
F
Invaded cells
C
DOC
dmr
Comb
G
C
DOC
dmr
Comb
H
Colonies
C
DOC
dmr
Comb
I
C
DOC
dmr
Comb
AR
AR-V7
β-actin
VEGF
PPARγ
pPPARγ
Sp1
β-actin
Bcl-2
Bax
α-tubulin
β-actin
J
Relative protein levels
AR
AR-V7
VEGF
PPAR-γ
p-PPARγ
Sp1
Bcl-2
Bax
α-tubulin
C
DOC
dmr
Comb

Figure 3. Effect of double mutated recombinant (dmr)FABP5 on the tumor-suppressive activity of docetaxel and relevant regulators in 22RV1 cells. (A) Effect on cell viability produced by a fixed dose of dmrFABP5 combined with different doses of docetaxel as a percentage of the control after 72 h. (B) Effect on cell viability produced by a fixed dose of docetaxel combined with different doses of dmrFABP5 as a percentage of the control after 72 h. (C) Effect of dmrFABP5 combined with docetaxel on cell migration in wound healing at 72 h (magnification: 20×) and (D) Quantitative assessment in terms of the percentage of original width of the wound. (E) Effect of dmrFABP5 combined with docetaxel on cell invasion at 24 h (magnification: 40×) and (F) Quantitative assessment in terms of number of invaded cells. (G) Effect of dmrFABP5 combined with docetaxel on cell anchorage-independent growth of cells in soft agar for 21 days (colonies >250 μm in diameters were counted) and (H) Quantitative assessment of the number of cell colonies after 21 days. (I) Western blot analysis of the effect of dmrFABP5 combined with docetaxel on the levels of the protein regulators AR, AR-V7, vascular endothelial growth factor, PPARγ, phosphorylated PPARγ, Sp1, Bcl-2, Bax and α-tubulin. Levels of the proteins were first normalized to β-actin and then to the control. (J) Quantitative assessment of the relative levels of the protein regulator by densitometric measurement of the intensities of the protein bands on the blots. Each experiment was performed in triplicate and the data are presented as the mean ± standard error of the mean. Student's t-test was used to compare the means. $P<0.05$ was considered to indicate a statistically significant difference. $^{*}P<0.05$, $^{**}P<0.001$, $^{***}P<0.0001$, $^{****}P<0.00001$. C, control; dmr, dmrFABP5 or double mutated recombinant FABP5; DOC, docetaxel; Com, combination of dmr and DOC; FABP5, fatty acid-binding protein 5; PPARγ, peroxisome proliferator-activated receptor; AR, androgen-receptor.

Table 3. Combination Index (CI) analysis for dmrFABP5 combined with docetaxel in 22RV1 cells

A. Fixed concentration of dmrFABP5 combined with different concentrations of docetaxel					
Cell lines	Dmr, μM	Docetaxel, nM	Suppression %	CI values	Relationship
22RV1	10	4	88	0.06834	Synergistic
22RV1	10	0.4	78	0.61895	Synergistic
22RV1	10	0.04	53	0.81263	Synergistic
22RV1	10	0.004	52	0.71955	Synergistic
B. Fixed concentration of docetaxel combined with different concentrations of dmrFABP5					
Cell lines	Dmr, μM	Docetaxel, nM	Suppression %	CI values	Relationship
22RV1	0.5	4	31	7.43467	Not synergistic
22RV1	1	4	59	0.38839	Synergistic
22RV1	5	4	66	0.53598	Synergistic
22RV1	10	4	89	0.07239	Synergistic

maximum suppression) and 0.88896, respectively (**Table 4A**). There was no synergistic suppression of dmrFABP5 at 10 μM combined with enzalutamide at 1 μM (CI=1.21405). However, a synergistic effect was found (**Figure 6B**) when the dose of enzalutamide was fixed at 10 μM and dmrFABP5 was added at 10, 5 and 1 μM, which produced reductions of 81, 62 and 44%, respectively, compared to 58, 46 and 26%, respectively, for dmrFABP5 alone. Enzalutamide at 10 μM in combination with dmrFABP5 at 0.5 μM did not produce a synergistic effect (CI=1.49663) (**Table 4B**).

Further investigations were performed on LNCaP cells (**Figure 7**). When the dose of dmrFABP5 was fixed at 20 μM and it was combined with enzalutamide (**Figure 7A**) at 1, 0.1, 0.01 and 0.001 μM, cell proliferation was inhibited by 80, 49, 32 and 6%, respectively, compared to 79, 48, 34 and 7%, respectively, for enzalutamide alone, yielding CIs that showed no synergy. Similarly, when a fixed dose of enzalutamide at 0.1 μM was combined with dmrFABP5 at 20, 10, 5 and 1 μM (**Figure 7B**), cell proliferation was inhibited by 45, 47, 44 and 47%, respectively, compared to 6, 5, 3 and 5%, respectively, for dmrFABP5 alone, yielding CIs that showed no synergy.

Effect of dmrFABP5 in combination with docetaxel or enzalutamide on the malignant characteristics of PC cells

Motility assay: Du145 cells were treated with DMSO as control for 24 h, the wound was almost completely closed (0%) (**Figure 2C**, **2D**). When treated with 3 nM docetaxel or 5 μM dmrFABP5 (**Figure 2C**), the width of the remaining wound was reduced to 70 or 82%, respectively, of that of the original wound. Whereas after 24 h, the wound width was 37 or 51%,

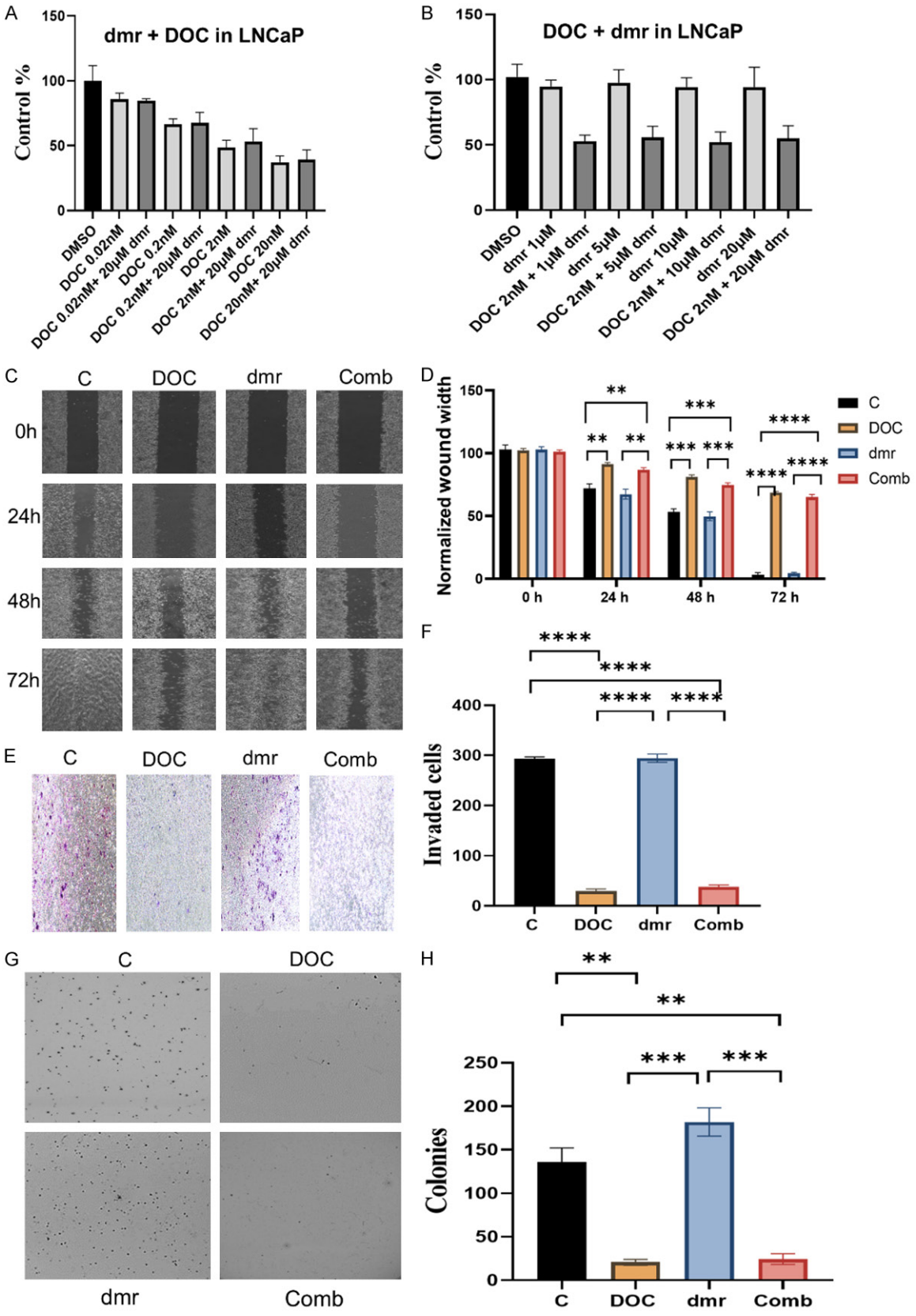

Figure 4. Effect of dmrFABP5 on the tumor-suppressive activity of docetaxel in LNCaP cells. (A) Effect on cell viability produced by a fixed dose of dmrFABP5 combined with different doses of docetaxel as a percentage of the control at 72 h. (B) Effect on cell viability produced by a fixed dose of docetaxel combined with different doses of dmrFABP5

as a percentage of the control. (C) Effect of dmrFABP5 combined with docetaxel on cell migration in wound healing (magnification: 20×) and (D) Quantitative assessment in terms of the percentage of the average width of the wound remaining after 72 h. (E) Effect of dmrFABP5 combined with docetaxel on cell invasion (magnification: 40×) and (F) Quantitative assessment of the average number of invaded cells at 24 h. (G) Effect of dmrFABP5 combined with docetaxel on anchorage-independent growth of cells in soft agar for 21 days (colonies with diameters >150 μm were counted) and (H) Quantitative assessment of the number of cell colonies after 21 days. Each experiment was performed in triplicate and the data are presented as the mean ± standard error of the mean. Student's t-test was used to compare the paired means. No multiple group comparison was conducted. P<0.05 was considered to indicate a statistically significant difference. *P<0.05, **P<0.001, ***P<0.0001, ****P<0.00001. C, control; dmr (double mutated recombinant FABP5), dmrFABP5; DOC, docetaxel; Com, combination of dmr and DOC; FABP5, fatty acid-binding protein 5.

respectively, of the original width. Inhibition was statistically significant at both inhibitions compared to the control groups (Student's t-test, P<0.05) (**Figure 2D**). The combination of both agents produced significantly wider wounds (Student's t-test, P<0.05) than those produced by either agent alone; with widths of 96 and 93% compared to that of the original wound (100%) after 12 and 24 h, respectively.

The same treatments were used on 22RV1 cells; DMSO was used for the control, and either docetaxel at 4 nM, dmrFABP5 at 10 μM or both compounds in combination were employed at different times (0, 24, 48 and 72 h) (**Figure 3C**). After 24 h, the gap widths were 60, 77, 79 and 96%, respectively, of the width of the original wound; this proved not to be significant (Student's t-test, P>0.05). Whereas after 48 h, the wound width was 49, 70, 69 and 92%, respectively, of the original wound. After 72 h, the widths were 20, 37, 40 and 89%, respectively. There was a significant difference in inhibition for each drug alone and in combination compared to the control, and the combination over the total inhibition by the 2 agents separately after 72 h (Student's t-test, P<0.001) (**Figure 3D**).

For LNCaP cells (**Figure 4C**), the same treatments were applied; DMSO control, 2 nM docetaxel, 20 μM dmrFABP5 and a combination of both drugs. After 24 h, the gap widths were 72, 69, 91 and 87%, respectively, of the widths of the original wounds. After 48 h, the gap widths were 53, 50, 81 and 79%, respectively, of the widths of the original wounds. After 72 h, the gaps widths were 3, 4, 69 and 65%, respectively, of those of the original wounds. At all times, docetaxel significantly inhibited wound closure (P<0.001), but dmrFABP5 failed to do so or to exert a significant effect on the combination of these drugs (P>0.05) (**Figure 4D**).

Further treatments were used when dmrFABP5 was combined with enzalutamide and their suppressive effects were investigated on Du145, 22RV1 and LNCaP cells. When Du145 cells were treated with DMSO, 100 μM enzalutamide, 5 μM dmrFABP5 or a combination of these drugs (**Figure 5C**), the gap widths after 12 h were 46, 47, 89 and 90%, respectively, while after 24 h, the gap widths were 5, 3, 78 and 76%, respectively. There was no significant effect with enzalutamide treatment compared to the control (Student's t-test, P>0.05), but a significant inhibition was observed with dmrFABP5 alone (P<0.0001) without further significant inhibition when in combination (**Figure 5D**).

22RV1 cells were treated with DMSO, 10 μM enzalutamide, 10 μM dmrFABP5 or a combination of both drugs (**Figure 6C**). The gap widths after 24 h were 74, 76, 88 and 97%, respectively. After 72 h, the gap widths were 33, 37, 69 and 91%, respectively, of the original width (**Figure 6D**). There was no significant inhibitory effect compared with the control after treatment with enzalutamide (P>0.05). However, at 72 h, dmrFABP5 showed a significant inhibition (P<0.001), which was further significantly increased when used in combination (P< 0.00001).

When LNCaP cells were treated for 24 h with DMSO, 100 nM enzalutamide, 20 μM dmrFABP5 or a combination of these drugs (**Figure 7C**), the gap widths were 74, 91, 71 and 86%, respectively, while after 48 h, the gap widths were 48, 91, 51 and 86%, respectively. After 72 h, the gap widths were 7, 65, 9 and 63%, respectively. Thus there was no significant effect over the control for dmrFABP5 treatment (P>0.05). However, enzalutamide alone showed significant inhibition at all times (P<0.05), but without any enhancement when used in combination with dmrFABP5 (P>0.05) (**Figure 7D**).

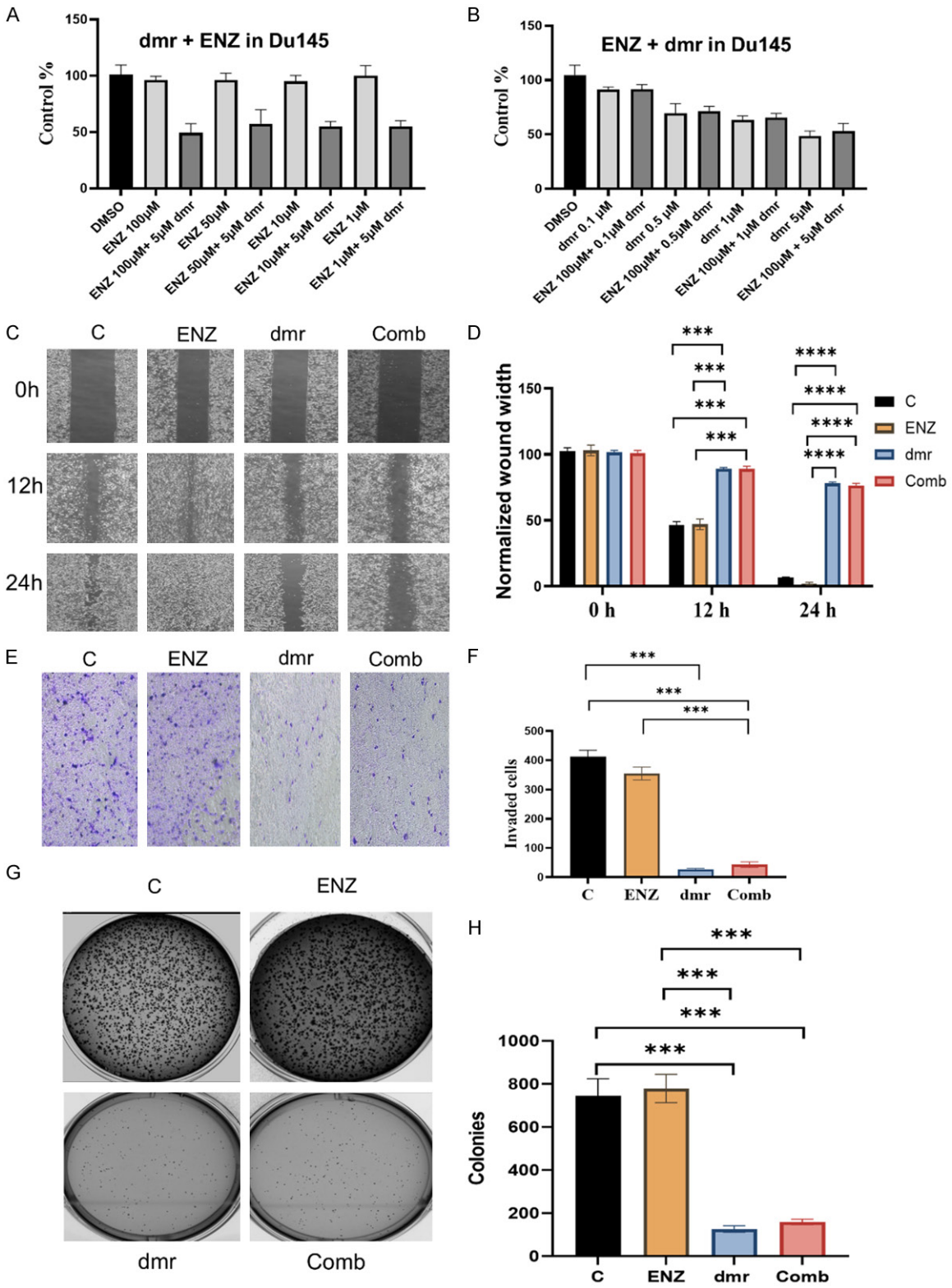

Figure 5. Effect of dmrFABP5 on the tumor-suppressive activity of enzalutamide in Du145 cells. (A) Effect on cell viability produced by a fixed dose of dmrFABP5 combined with different doses of enzalutamide as a percentage of the control at 72 h. (B) Effect on cell viability produced by a fixed dose of enzalutamide combined with different doses of dmrFABP5 as a percentage of the control at 72 h. (C) Effect of dmrFABP5 combined with enzalutamide on cell migration in wound healing assay at 72 h (magnification: 20×) and (D) Quantitative assessment in terms of the percentage of the original width of the wound remaining at different time points. (E) Effect of dmrFABP5 combined

with enzalutamide on cell invasion at 24 h and (F) Quantitative assessment of the number of cells at 24 h (magnification: 20×). (G) Effect of dmrFABP5 combined with enzalutamide on anchorage-independent growth of cells in soft agar at 21 days (colonies with diameters >250 μm were counted) and (H) Quantitative assessment of the number of cell colonies in soft agar after 21 days. Each experiment was performed in triplicate and the data are presented as the mean ± standard error of the mean. Student's t-test was used to compare the paired means. No multiple group tests were conducted. P<0.05 was considered to indicate a statistically significant difference. *P<0.05, **P<0.001, ***P<0.0001, ****P<0.00001. C, control; ENZ, enzalutamide; dmr, dmrFABP5; Com, combination of dmr and ENZ; FABP5, fatty acid-binding protein 5.

Invasion assay: When Du145 cells were treated with control DMSO, docetaxel, dmrFABP5 or a combination of these drugs at the same concentrations as those used in the motility assay to evaluate their invasiveness after 24 h (**Figure 2E**), the mean ± SEM number of invaded cells was 449±14, 89±3, 68±3 and 9±1, respectively, resulting in suppressions by 0% (control), -80%, 82%, and 98%, respectively, versus the control (**Figure 2F**). Thus, not only did both agents alone significantly inhibit invasion (P<0.0001), but also their combination significantly enhanced the effect of either agent alone (P<0.0001).

Next, 22RV1 cells were treated with similar concentrations to those employed in the motility assays. Upon treatment with DMSO, docetaxel, dmrFABP5 or a combination of both drugs (**Figure 3E**), the mean ± SEM number of invaded cells was 306±7, 88±3, 110±3 and 14±2, respectively, leading to suppressions by 0% (control), 71, 64 and 93%, respectively versus the control. Thus, each single agent alone significantly suppressed cell invasion (P<0.0001), although the combination significantly enhanced suppression compared to the effect of each single agent (P<0.001) (**Figure 3F**).

When LNCaP cells were treated with DMSO, docetaxel, dmrFABP5 or a combination of both drugs at the same concentrations used in the motility assay (**Figure 4E**), the mean ± SEM number of invaded cells was 29±4, 294±9, 29±4 and 37±5, respectively. There was a significant difference between the docetaxel and control groups (P<0.001), but there was no significant difference for dmrFABP5 alone or in combination versus the control (P>0.05) (**Figure 4F**).

When Du145 cells were treated with DMSO, enzalutamide, dmrFABP5 or a combination of both drugs at the same doses used in motility assays (**Figure 5E**), the mean ± SEM number of invaded cells was 425±26, 413±21, 27±2 and 43±10, respectively. Enzalutamide failed to inhibit cell invasion significantly (P>0.05), whereas dmrFABP5 caused a significant suppression (P<0.0001), although the drug combination had no significant enhancement effect (P>0.05) (**Figure 5F**).

When 22RV1 cells were treated with DSMO, enzalutamide, dmrFABP5 or a combination of these drugs at the same concentrations as those used in motility assays (**Figure 6E**), the mean ± SEM number of invaded cells was 292±33, 321±10, 80±11 and 8±1, respectively. There was no significant difference in the enzalutamide alone group (P>0.05), but a significant difference was observed for dmrFABP5 versus the control (P<0.001) and for combined treatment versus dmrFABP5 alone (P<0.001) (**Figure 6F**).

When LNCaP cells were treated with DMSO, enzalutamide, dmrFABP5 or a combination of both drugs at the same concentrations as those used in motility assays (**Figure 7E**), the mean ± SEM number of invaded cells was 315±22, 310±42, 60±3 and 73±9, respectively. Enzalutamide significantly inhibited cell invasion compared to the control (P<0.0001), but dmrFABP5 failed to do so, and a combination of both agents failed to inhibit the invasion caused by enzalutamide alone (P>0.05) (**Figure 7F**).

Soft agar assay: When Du145 cells were treated with control DMSO, docetaxel, dmrFABP5 or both drugs in combination at the same concentrations as those used in motility assays (**Figure 2G**), the mean number of colonies ± SEM was 880±44, 144±37, 217±33 and 16±4, respectively. Docetaxel and dmrFABP5 alone significantly inhibited colony formation (P<0.0001) and their combination caused a further significant inhibition (P<0.0001) (**Figure 2F**).

When 22RV1 cells were treated with control DMSO, docetaxel, dmrFABP5 or a combination

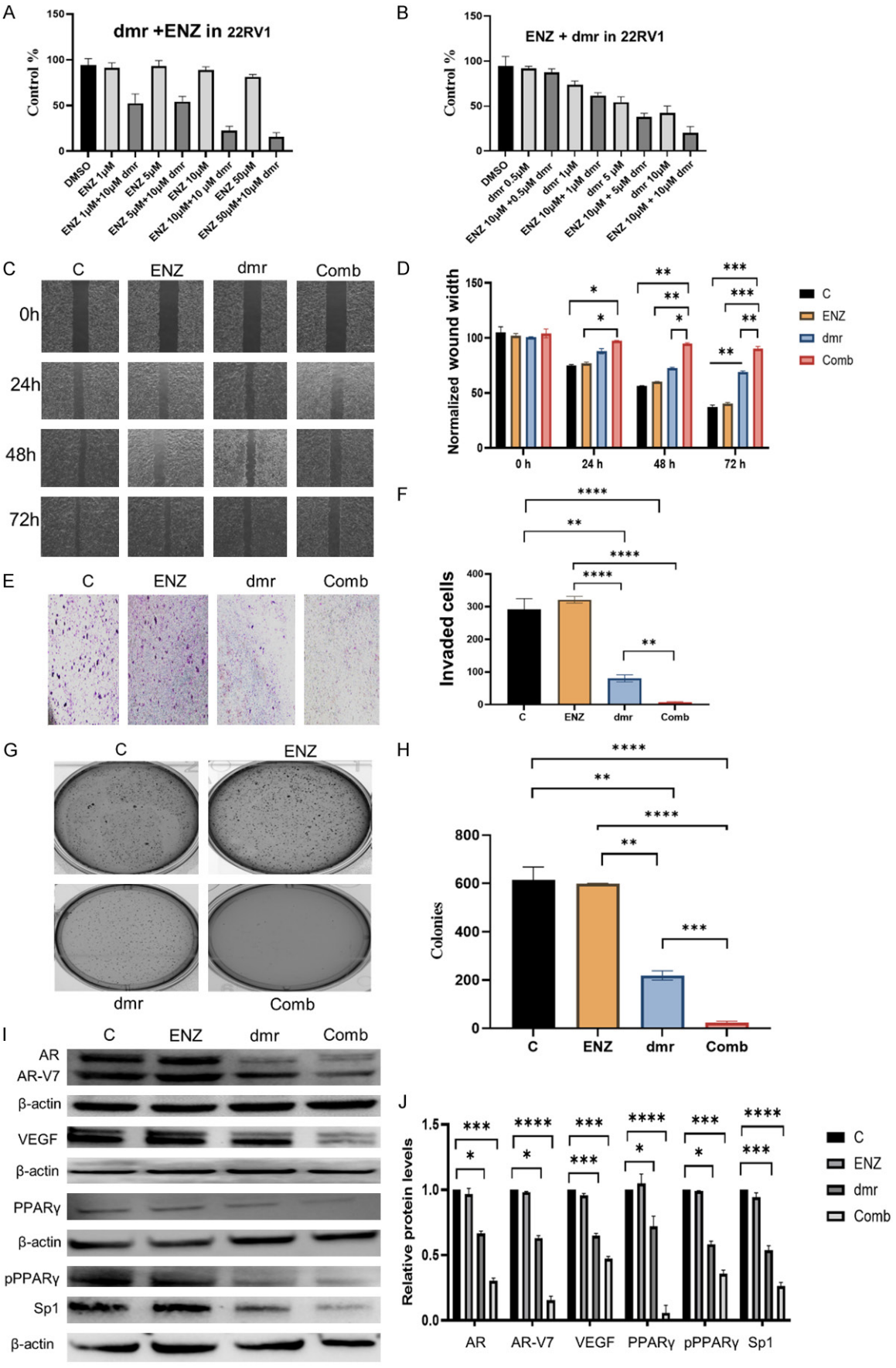
A
dmr +ENZ in 22RV1
Control %
DMSO
ENZ 1μM
ENZ 1μM+10μM dmr
ENZ 5μM
ENZ 5μM+10μM dmr
ENZ 10μM
ENZ 10μM+10 μM dmr
ENZ 50μM
ENZ 50μM+10μM dmr
B
ENZ + dmr in 22RV1
Control %
DMSO
dmr 0.5μM
ENZ 10μM +0.5μM dmr
dmr 1μM
ENZ 10μM+ 1μM dmr
dmr 5 μM
ENZ 10μM + 5μM dmr
dmr 10μM
ENZ 10μM + 10μM dmr
C
C
ENZ
dmr
Comb
0h
24h
48h
72h
D
Normalized wound width
0 h
24 h
48 h
72 h
C
ENZ
dmr
Comb
E
C
ENZ
dmr
Comb
F
Invaded cells
C
ENZ
dmr
Comb
G
C
ENZ
dmr
Comb
H
Colonies
C
ENZ
dmr
Comb
I
C
ENZ
dmr
Comb
AR
AR-V7
β-actin
VEGF
β-actin
PPARγ
β-actin
pPPARγ
Sp1
β-actin
J
Relative protein levels
AR
AR-V7
VEGF
PPARγ
pPPARγ
Sp1
C
ENZ
dmr
Comb

Figure 6. Effect of dmrFABP5 on the tumor-suppressive activity of enzalutamide and relevant regulators in 22RV1 cells. (A) Effect on cell viability produced by a fixed dose of dmrFABP5 combined with different doses of enzalutamide as a percentage of the control at 72 h. (B) Effect on cell viability produced by a fixed dose of enzalutamide combined with different doses of dmrFABP5 as a percentage of the control at 72 h. (C) Effect of dmrFABP5 combined with enzalutamide on cell migration in wound healing at different time points (magnification: 20×) and (D) Quantitative assessment in terms of the width of the remaining wound expressed as a percentage of the original width at different time points. (E) Effect of dmrFABP5 combined with enzalutamide on the cell invasion at 24 h (magnification: 40×) and (F) Quantitative assessment of the number of invaded cells after 24 h. (G) Effect of dmrFABP5 combined with enzalutamide on cell anchorage-independent growth in soft agar at 21 days and (H) Quantitative assessment of the number of cell colonies in soft agar at 21 days. Colonies with diameters >250 μm were counted. (I) Western blot analysis of the effect of dmrFABP5 combined with enzalutamide on the expression levels of protein regulators. (J) Quantitative assessment of the Western blot results for AR, AR-V7, vascular endothelial growth factor, PPARγ, phosphorylated PPARγ and Sp1. The relative protein levels were obtained by densitometrical scanning of peak areas of the bands on the blot, which were normalized first to β-actin and then to the control. Each experiment was performed in triplicate and the data are presented as the mean ± standard error of the mean. Student's t-test was used to compare the paired means. No multiple group tests were conducted. $P<0.05$ was considered to indicate a statistically significant difference. $^{*}P<0.05$, $^{**}P<0.001$, $^{***}P<0.0001$, $^{****}P<0.00001$. C, control; ENZ, enzalutamide; dmr, dmrFABP5; Com, combination of dmr and ENZ; FABP5, fatty acid-binding protein 5; PPARγ, peroxisome proliferator-activated receptor; AR, androgen-receptor.

Table 4. Combination Index (CI) analysis for dmrFABP5 combined with enzalutamide in 22RV1 cells

A. Fixed concentration of dmrFABP5 combined with different concentrations of enzalutamide					
Cell lines	Dmr, μM	Enzalutamide, nM	Suppression %	CI values	Relationship
22RV1	10	50	84	0.1447	Synergistic
22RV1	10	10	77	0.1084	Synergistic
22RV1	10	5	65	0.8881	Synergistic
22RV1	10	1	55	0.8340	Synergistic
B. Fixed concentration of enzalutamide combined with different concentrations of dmrFABP5					
Cell lines	Dmr, μM	Enzalutamide, nM	Suppression %	CI values	Relationship
22RV1	0.5	10	11	1.4963	Not synergic
22RV1	1	10	42	0.8611	Synergistic
22RV1	5	10	62	0.2321	Synergistic
22RV1	10	10	80	0.1136	Synergic

The combination index (CI) values were calculated using CompuSyn software, and the result is considered to be synergistic when CI<0.9.

of both agents at the same concentrations as those used in motility assays (**Figure 3G**), the mean number of the colonies ± SEM was 621±30, 119±11, 354±28 and 18±5, respectively. Docetaxel and dmrFABP5 significantly inhibited colony formation when used alone ($P<0.001$), and their combination caused a further significant inhibition ($P<0.001$) (**Figure 3F**).

When LNCaP cells were treated with control DMSO, docetaxel, dmrFABP5 or a combination of both agents at the same concentrations as those used in motility assays (**Figure 4G**), the mean number of colonies ± SEM was 290±12, 62±9, 299±45 and 69±10, respectively. Only docetaxel produced a significant decrease in colony formation compared to the control ($P<0.001$), while dmrFABP5 failed to do so ($P>0.05$). The combination of both agents caused no further decrease ($P>0.001$) (**Figure 4H**).

When Du145 cells were treated with control DMSO, enzalutamide, dmrFABP5 or a combination of both agents at the same concentrations as those used in motility assays (**Figure 5G**), the mean number of colonies ± SEM was 778±66, 743±81, 113±9 and 159±12, respectively. Enzalutamide produced no significant decrease in colony formation ($P>0.05$), whereas dmrFABP5 did so ($P<0.0001$). However, there was no further decrease with a combination of both agents ($P>0.05$) (**Figure 5H**).

When 22RV1 cells were treated with control DMSO, enzalutamide, dmrFABP5 or a combination of both agents at the same concentrations as those used in motility assays (**Figure 6G**),

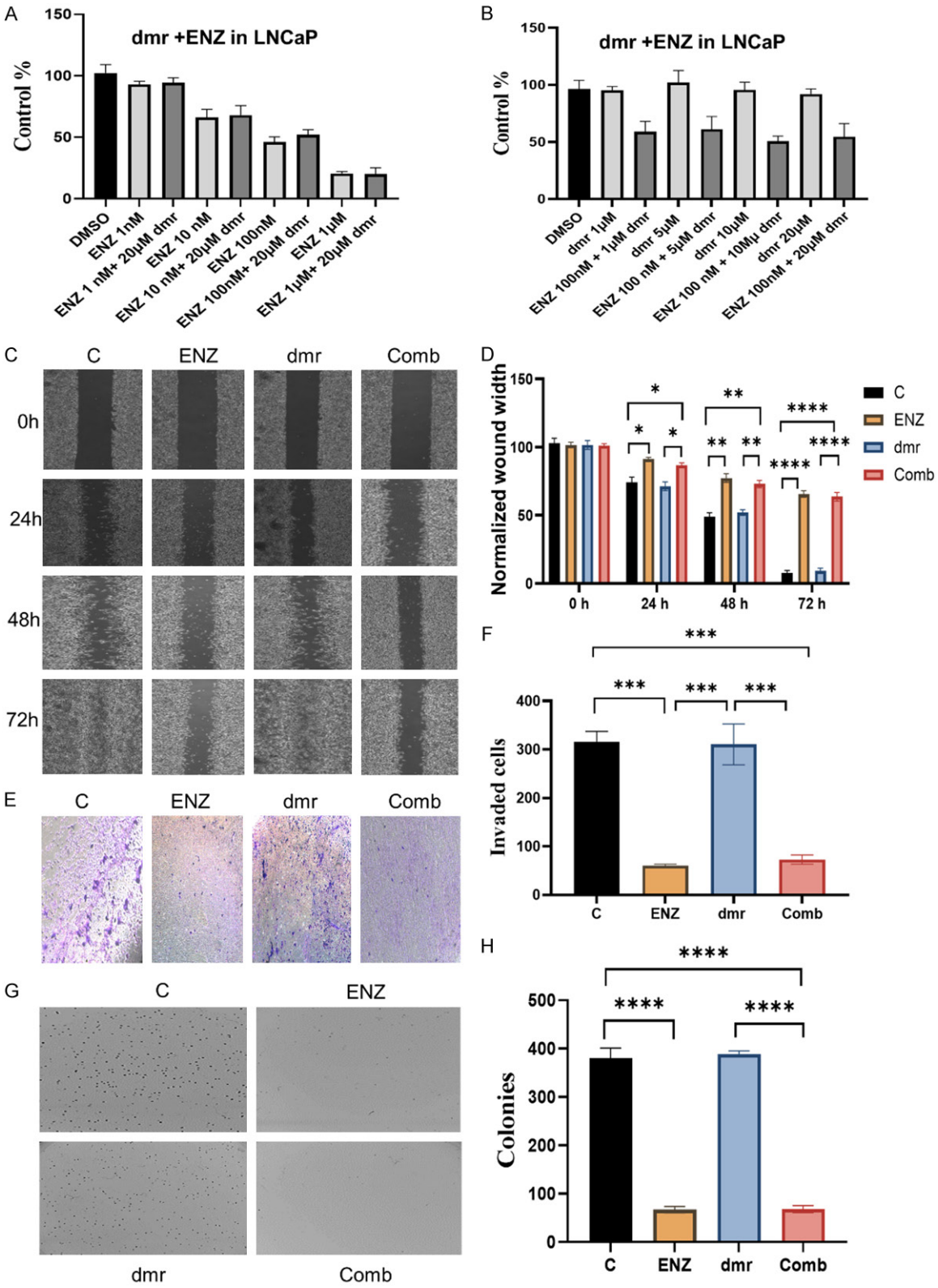

Figure 7. Effect of dmrFABP5 on the tumor-suppressive activity of enzalutamide in LNCaP cells. (A) Effect on cell viability produced by a fixed dose of dmrFABP5 combined with different doses of enzalutamide as a percentage of the control at 72 h. (B) Effect on cell viability produced by a fixed dose of enzalutamide combined with different doses of dmrFABP5 as a percentage of the control at 72 h. (C) Effect of dmrFABP5 combined with enzalutamide on cell migration in wound healing assay at different time points (magnification: 20×) and (D) Quantitative assessment in terms of average the width of the wound remaining, expressed as a percentage of the original width after different

time points. (E) Effect of dmrFABP5 combined with enzalutamide on cell invasion after 24 h. Magnification: 40×. (F) Quantitative assessment of the number of invaded cells after 24 h. (G) Effect of dmrFABP5 combined with enzalutamide on anchorage-independent growth of cells in soft agar at 21 days. Colonies with diameters >150 μm were counted. (H) Quantitative assessment of the number of cell colonies at 21 days. Each experiment was performed in triplicate and the data are presented as the mean ± standard error of the mean. Student's t-test was used to compare the paired means. No multiple group tests were conducted. P<0.05 was considered to indicate a statistically significant difference. *P<0.05, **P<0.001, ***P<0.0001. C, control; ENZ, enzalutamide; dmr, dmrFABP5; Com, combination of dmr and ENZ; FABP5, fatty acid-binding protein 5.

the mean number of colonies ± SEM was 614±54, 599±6.75, 219±19 and 23±6, respectively. Enzalutamide produced no significant decrease in colony formation (P>0.05), while dmrFABP5 did so (P<0.001), and there was a further significant decrease with a combination of both agents (P<0.001) (**Figure 6H**).

When LNCaP cells were treated with control DMSO, enzalutamide, dmrFABP5 or a combination of both drugs at the same concentrations as those used in motility assays (**Figure 7G**), the mean number of colonies ± SEM was 380±21, 67±6, 394±26 and 68±7, respectively. Enzalutamide significantly inhibited colony formation (P<0.0001), whereas dmrFABP5 did not (P>0.05), and there was no further significant decrease with the combination of both agents (P>0.05) (**Figure 7H**).

Molecular mechanism involved in combination treatments

When Du145 cells were treated with control DMSO, docetaxel, dmrFABP5 or both drugs in combination at concentrations used in previous assays (**Figure 2I**), the relative levels of VEGF protein determined by Western blotting were 1, 0.64±0.03, 0.60±0.06 and 0.35±0.01, respectively. Docetaxel or dmrFABP5 alone produced a significant decrease in VEGF compared to the control (P<0.05), and in combination they triggered a further significant decrease in VEGF levels (P<0.001) (**Figure 2J**).

Similarly, when DU145 cells were treated with control DMSO, docetaxel, dmrFABP5 or both drugs in combination at concentrations used in previous assays (**Figure 2I**), Western blotting revealed that the relative levels of PPARγ and p-PPARγ were 1 and 1, 0.96±0.02 and 0.75±0.01, 0.44±0.01 and 0.65±0.01, and 0.22±0.01 and 0.26±0.01, respectively. Upon docetaxel treatment, there was no significant change in PPARγ levels (P>0.05), while dmrFABP5 treatment caused a significant reduction in PPARγ (P<0.001) and p-PPARγ levels (P<0.05). The combination of both agents caused a further significant reduction in PPARγ (P<0.01) and p-PPARγ (P<0.001) levels compared to the effect caused by either agent alone (**Figure 2J**).

When Du145 cells were treated as described above manner and evaluated by Western blotting, the relative levels of α-tubulin were 1, 1.928±0.003, 1.733±0.03 and 2.384±0.09, respectively. Both docetaxel and dmrFABP5 significantly increased α-tubulin levels (P< 0.001), and their combination triggered a further significant increase in α-tubulin levels (P<0.0001) (**Figure 2J**).

When Du145 cells were treated as aforementioned and subjected to western blotting (**Figure 2I**), the relative levels of Sp1 were 1, 0.46±0.07, 0.57±0.02 and 0.12±0.03, respectively. Both docetaxel (P<0.001) and dmtFABP5 (P<0.01) alone significantly reduced Sp1 levels, and in combination they triggered a further significant reduction in Sp1 levels (P<0.0001) (**Figure 2J**).

When Du145 cells were treated with control DMSO, docetaxel, dmrFABP5 or a combination of both drugs, and then evaluated by Western blotting, the levels of Bcl-2 were 1, 0.37±0.02, 0.49±0.04 and 0.13±0.3, respectively. Both docetaxel and dmrFABP5 alone significantly reduced Bcl-2 levels (P<0.001), and in combination they triggered a further significant reduction in Bcl-2 levels (P<0.0001) (**Figure 2J**).

When Du145 cells were treated with control DMSO, docetaxel, dmrFABP5 or in combination and subjected to Western blotting, the levels of Bax were 1, 1.83±0.06, 2.63±0.047 and 3.3±0.09, respectively. Both docetaxel and dmrFABP5 alone significantly increased Bax levels (P<0.01 and P<0.001, respectively), and their combination triggered a further significant increase in Bax levels (P<0.0001) (**Figure 2J**).

When 22RV1 cells were treated with control DMSO, docetaxel, dmrFABP5 or in combination at the same concentrations as those used in previous assays and subjected to Western blotting (**Figure 3I**), the relative levels of AR and AR-V7 were 1 and 1, 0.68±0.03 and 0.34±0.02, 0.78±0.02 and 0.57±0.3, and 0.25±0.04 and 0.09±0.01, respectively (**Figure 3J**). Docetaxel or dmrFABP5 alone significantly reduced AR or AR-V7 ($P<0.001$ and $P<0.01$, respectively), while their combination triggered further significant reductions in both AR and AR-V7 ($P<0.0001$ and $P<0.00001$, respectively).

When 22RV1 cells were treated with control DMSO, docetaxel, dmrFABP5 or a combination of both drugs at the same concentrations as those used in previous assays, and the cells were evaluated by Western blotting (**Figure 3I**), the relative levels of VEGF were 1, 0.49±0.08, 0.41±0.03 and 0.03±0.01, respectively. Both docetaxel and dmrFABP5 led to significantly reduced VEGF levels ($P<0.01$ and $P<0.0001$, respectively), and in combination they triggered a further significant reduction ($P<0.00001$) (**Figure 3J**).

When 22RV cells were treated with DMSO, docetaxel, dmrFABP5 or a combination of both drugs, the relative levels of PPARγ and p-PPARγ were 1 and 1, 0.77±0.02 and 0.75±0.06, 0.84±0.01 and 0.63±0.01, and 0.62±0.01 and 0.46±0.02, respectively. Both docetaxel and dmrFABP5 significantly reduced PPARγ and p-PPARγ levels (both $P<0.05$), and in combination they triggered a further significant reduction ($P<0.01$ and $P<0.001$, respectively) (**Figure 3J**).

When 22RV1 cells were treated with DMSO, docetaxel, dmrFABP5 or a combination of both drugs (**Figure 3I**), the relative level of Sp1 was 1, 0.35±0.04, 0.63±0.05 and 0.11±0.01, respectively (**Figure 3J**). Either agent alone significantly reduced the Sp1 levels ($P<0.01$ and $P<0.001$, respectively), and in combination they triggered a further significant reduction in Bax levels ($P<0.001$).

When 22RV1 cells were treated with DMSO, docetaxel, dmrFABP5 or a combination of both drugs (**Figure 3I**), the relative levels of Bcl-2 and Bax were 1 and 1, 0.45±0.05 and 1.84±0.05, 0.61±0.04 and 1.4±0.05, and 0.14±0.01 and 3.15±0.25, respectively (**Figure 3J**). Both docetaxel and dmtFABP5 alone significantly reduced Bcl-2 levels ($P<0.01$ and $P<0.05$, respectively), and significantly increased Bax levels ($P<0.01$ and $P<0.05$, respectively), while their combination triggered a further significant Bcl-2 reduction ($P<0.00001$) and Bax increase ($P<0.00001$).

When 22RV1 cells were treated with DMSO, docetaxel, dmrFABP5 or a combination of both drugs (**Figure 3I**), the relative levels of α-tubulin were 1, 2.40±0.17, 2.15±0.25 and 2.8±0.04, respectively. Both docetaxel and dmrFABP5 separately increased α-tubulin significantly ($P<0.001$ and $P<0.001$, respectively), but in combination they did not produce a significant further increase ($P>0.05$).

When 22RV1 cells were treated with DMSO, enzalutamide, dmrFABP5 or a combination of both agents (**Figure 6I**), the relative levels of AR and AR-V7 were 1 and 1, 0.95±0.06 and 0.96±0.02, 0.74 ±0.01 and 0.41±0.06, and 0.28±0.02 and 0.18±0.01, respectively (**Figure 6J**). Enzalutamide failed to reduce AR or AR-V7 levels significantly ($P>0.05$), while dmrFABP5 did so ($P<0.01$), and in combination they triggered a significant further reduction in AR ($P<0.0001$) and AR-V7 ($P<0.00001$) levels.

When 22RV1 cells were treated with DMSO, enzalutamide, dmrFABP5 or a combination of both drugs (**Figure 6I**), the relative levels of VEGF were 1, 0.95±0.10, 0.59±0.06 and 0.23± 0.03, respectively. Enzalutamide failed to reduce VEGF levels significantly ($P>0.05$), while dmrFABP5 did so ($P<0.001$), and their combination triggered a further significant reduction ($P<0.0001$) (**Figure 6J**).

When 22RV1 cells were treated with DMSO, enzalutamide, dmrFABP5 or a combination of both drugs (**Figure 6I**), the relative levels of PPARγ and p-PPARγ were 1 and 1, 1.05±0.05 and 0.91±0.02, 0.77±0.01 and 0.58±0.01, and 0.28±0.04 and 0.29±0.05, respectively. Enzalutamide failed to reduce PPARγ or p-PPARγ levels significantly ($P>0.05$), while dmrFABP5 did so ($P<0.001$), and their combination triggered a further significant reduction in PPARγ or p-PPARγ levels (both $P<0.0001$).

When 22RV1 cells were treated with DMSO, enzalutamide, dmrFABP5 or a combination of both drugs (**Figure 6I**), the relative levels of Sp1

were 1, 0.94±0.02, 0.56±0.62 and 0.21±0.03, respectively. Enzalutamide failed to decrease Sp1 levels significantly ($P>0.05$), but dmrFABP5 did so ($P<0.0001$), and their combination triggered a further significant decrease in Sp1 levels ($P<0.00001$) (**Figure 6J**).

Discussion

PC is a common cancer type in male patients and a leading cause of cancer-associated mortalities. Treatment typically involves ADT, but a more aggressive form of PC called CRPC can develop, which is resistant to ADT [47]. The molecular mechanism involved in the transition of the cancer cells from androgen-dependent to androgen-independent state is not well understood. Currently, the dominant theory is that, under the high selection pressure during the first round of ADT, the biological sensitivity of AR is amplified (due to mutations and/or differential RNA splicing) to such an extent that even microquantities of the remaining male hormone in peripheral blood can still be used to promote the malignant progression of CRPC cells [48]. Thus, in the clinic, further ADT is generally prescribed, thereby potentially increasing the ability of the drug to block microquantities of male hormones, even though the effectiveness of ADT remains inconclusive or even controversial. These treatments include recent anti-androgen or AR-targeting drugs, such as abiraterone and enzalutamide [42, 49]. Therefore, it has been suggested that ADT can eventually lead to a therapeutic deed end with little benefit for patients [50-52].

An alternative theory is based on our previous studies that have shown that FABP5 interacts with PPARγ which in turn stimulates VEGF and other factors that promote properties associated with the malignant state in PC [9, 10]. In this theory, it is the FABP5-PPARγ-VEGF axis, rather than the AR-related target Sp1, that is responsible for CRPC progression [10]. FABP5 itself can promote cell proliferation and metastasis by transporting fatty acids, thereby activating PPARγ and eventually increasing the downstream cancer-promoting genes [19]. Targeting FABP5 with inhibitors such as dmrFABP5 or SB-FI-26 has shown promise either in inhibiting the malignant progression of PC cells or in increasing their sensitivity to apoptosis induction [16, 17]. Moreover, treatment of PC with enzalutamide or docetaxel eventually loses effectiveness due to resistance to these drugs, with the development of AR-V7 being a major factor, since knocking down AR-V7 re-sensitise cells to anti-androgen treatments [53-55]. The present study investigated a combination therapy using dmrFABP5, together with docetaxel, or enzalutamide, to treat PC cells. Initially, the IC_{50} values of three compounds (dmrFABP5, docetaxel and enzalutamide) were determined in three PC cell lines (Du145, 22RV1 and LNCaP) to evaluate cell viability. In Du145 and 22RV1 cells, dmrFABP5 produced IC_{50} values of 5 and 12 μM, respectively, while no significant inhibition was observed in LNCaP cells. Docetaxel exhibited IC_{50} values of 3, 4 and 2.2 nM in Du145, 22RV1 and LNCaP cells, respectively. Enzalutamide showed no significant inhibition in LNCaP and 22RV1 cells. However, in LNCaP cells, the IC_{50} value of enzalutamide was 97 nM (**Figure 1**). These results clearly demonstrated that dmrFABP5 inhibited cell viability in FABP5-positive cells and had no effect on the FABP5-negative LNCaP cells. Docetaxel effectively suppressed the viability of PC cells, while enzalutamide did not suppress androgen-independent Du145 cells or androgen-responsive 22RV1 cells expressing LBD-negative AR-V7 receptor. Enzalutamide suppressed LNCaP cells, but these cells only expressed AR-FL and not AR-V7 [49, 53, 55]. When used in combination, dmrFABP5 and docetaxel demonstrated a strong synergistic effect, resulting in a maximum suppression of 89% in Du145 cells and 92% in 22RV1 cells. However, no synergistic interaction was observed in LNCaP cells. When dmrFABP5 was combined with enzalutamide, no synergistic effect was observed in Du145 cells, but a highly synergistic effect of 87% suppression of cell viability was observed in 22RV1 cells, although not in LNCaP cells (**Tables 2**-**4**; **Figure 7**).

Regarding cell migration, the combination of dmrFABP5 and docetaxel resulted in a significant 93% wound gap in Du145 cells, surpassing the individual effects of each compound alone (**Figure 2C** and **2D**). However, when dmrFABP5 was combined to enzalutamide to treat Du145 cells, there was no additional reduction in wound gap compared with the effect of dmrFABP5 alone (**Figure 5C** and **5D**). The combination of dmrFABP5 and docetaxel

demonstrated a significant suppression of cell migration in 22RV1 cells, achieving a maximum of 89% wound gap (**Figure 3C** and **3D**). This synergistic effect was greater than the effects of each agent alone. In 22RV1 cells, the combination of dmrFABP5 with enzalutamide resulted in 91% wound gap reduction, which was significantly higher than the effects of enzalutamide (37%) or dmrFABP5 alone (69%) (**Figure 6C** and **6D**). However, in LNCaP cells, the combination of dmrFABP5 with either docetaxel or enzalutamide did not enhance their individual effects, although treatments with either docetaxel or enzalutamide alone significantly inhibited cell migration, resulting in wound gaps of 69 and 65%, respectively (**Figures 4C**, **4D**, **7C** and **7D**).

Regarding cell invasion, dmrFABP5 synergistically enhanced the suppressive effect of docetaxel in Du145 cells, resulting in a 98% inhibition of cell invasion (**Figure 2E** and **2F**), but when dmrFABP5 was combined with enzalutamide, no additional suppression was observed (**Figure 5E** and **5F**). In 22RV1 cells, enzalutamide alone did not significantly suppress cell invasion, while dmrFABP5 alone achieved a 72% inhibition. The combination of dmrFABP5 with enzalutamide resulted in a significant 97% inhibition, indicating an enhancement effect compared with that of either agent alone (**Figure 6E** and **6F**). No enhancement was observed in LNCaP cells when dmrFABP5 was combined with docetaxel or enzalutamide, although both drugs individually significantly inhibited cell invasion (**Figures 4E**, **4F**, **7E** and **7F**).

Previous research on colony formation in agar revealed that dmrFABP5 was able to suppress colony formation in PC3-M cells [17]. In the present study, when combined with docetaxel, dmrFABP5 significantly enhanced the inhibition of colony formation in Du145 cells (**Figure 2G** and **2H**), but its combination with enzalutamide failed to produce a significant effect (**Figure 5G** and **5H**), indicating that enzalutamide did not function in AR-negative Du145 cells. In 22RV1 cells, the combination of dmrFABP5 with either docetaxel or enzalutamide showed a synergistic effect, resulting in greater suppression of colony formation compared with that caused by each compound alone (**Figures 3G**, **3H**, **6G** and **6H**). No significant enhancement was observed in LNCaP cells when the same combinations were used (**Figures 4G**, **4H**, **7E** and **7H**), suggesting that dmrFABP5 did not enhance the suppressive effect of docetaxel or enzalutamide in FABP5-negative cells.

The results of cell viability assays and of studies on cell properties associated with malignant progression, wound closure, cell invasion and growth in agar conducted in the present study are consistent. DmrFABP5 can function alone and synergise with docetaxel in Du145 and 22RV cells, and it synergises with enzalutamide only in 22RV1 cells, but it fails alone to inhibit or synergise with either inhibitory drug in LNCaP cells. Moreover, these biological effects were consistent with changes in the levels of proteins considered to be involved in their pathways, at least for dmrFABP5 and docetaxel (**Figure 3I** and **3J**). However, changes in individual pathways (FABP5→p-PPARγ→VEGF→angiogenesis and docetaxel→α-tubulin→Sp1→Bax, Bcl-2→apoptosis, respectively) appeared to overlap to a certain extent (**Figure 3I** and **3J**), perhaps also contributing to the overall changes in pathway proteins beyond those observed for either dmrFABP5 or docetaxel alone (**Figure 3I** and **3J**). Thus, the combination of dmrFABP5 with either docetaxel or enzalutamide could enhance the suppression of malignant properties in specific PC cell lines, whilst the lack of synergistic effects may be attributable to the absence of specific targets or the expression of certain proteins that no longer respond to these therapeutic agents.

In this study, we have demonstrated that the combination of dmrFABP5 with docetaxel synergistically suppresses FABP5-positive cells. The combination of dmrFABP5 with enzalutamide shows promising results in restoring sensitivity to enzalutamide, which was previously resistant due to AR-V7 expression. Changes in key proteins related to FABP5-initiated signalling pathways suggest that the observed synergistic effect is achieved through influencing this pathway and other pathways involving regulatory proteins such as Sp1, Bcl-2 and BAX measured here. Although these *in vitro* studies are at a preliminary stage, the results from this work form a solid basis for development of a new treatment strategy. In future studies, further tests in relevant animal models and other preclinical work will be needed before any possible clinical trials. The pres-

ent results combined with the previous findings that FABP5 is over expressed in >90% of prostate carcinomas [8] suggest that dmrFABP5 may be a potentially new therapeutic drug that can be developed as an agent to suppress the malignant progression of CRPC.

Acknowledgements

SAA and AAN were supported by PhD scholarships from King Saud Bin Abdulaziz University for Health Sciences, College of Science and Health Professions, Jeddah, Saudi Arabia. BTA is supported by a PhD studentship from the Faculty of Medicine, Northern Borders University, Saudi Arabia.

Disclosure of conflict of interest

None.

Address correspondence to: Youqiang Ke, Department of Molecular and Clinical Cancer Medicine, Liverpool University, CRC Building, No. 200 London Road, Liverpool L3 9TA, UK. E-mail: yqk@liverpool.ac.uk

References

[1] Sung H, Ferlay J, Siegel RL, Laversanne M, Soerjomataram I, Jemal A and Bray F. Global cancer statistics 2020: GLOBOCAN estimates of incidence and mortality worldwide for 36 cancers in 185 countries. CA Cancer J Clin 2021; 71: 209-249.

[2] Frieling JS, Basanta D and Lynch CC. Current and emerging therapies for bone metastatic castration-resistant prostate cancer. Cancer Control 2015; 22: 109-120.

[3] Deep G and Schlaepfer IR. Aberrant lipid metabolism promotes prostate cancer: role in cell survival under hypoxia and extracellular vesicles biogenesis. Int J Mol Sci 2016; 17: 1061.

[4] Zadra G, Photopoulos C and Loda M. The fat side of prostate cancer. Biochim Biophys Acta 2013; 1831: 1518-1532.

[5] Apte SA, Cavazos DA, Whelan KA and Degraffenried LA. A low dietary ratio of omega-6 to omega-3 Fatty acids may delay progression of prostate cancer. Nutr Cancer 2013; 65: 556-562.

[6] Levi L, Wang Z, Doud MK, Hazen SL and Noy N. Saturated fatty acids regulate retinoic acid signalling and suppress tumorigenesis by targeting fatty acid-binding protein 5. Nat Commun 2015; 6: 8794.

[7] Jing C, Beesley C, Foster CS, Rudland PS, Fujii H, Ono T, Chen H, Smith PH and Ke Y. Identification of the messenger RNA for human cutaneous fatty acid-binding protein as a metastasis inducer. Cancer Res 2000; 60: 2390-2398.

[8] Morgan EA, Forootan SS, Adamson J, Foster CS, Fujii H, Igarashi M, Beesley C, Smith PH and Ke Y. Expression of cutaneous fatty acid-binding protein (C-FABP) in prostate cancer: potential prognostic marker and target for tumourigenicity-suppression. Int J Oncol 2008; 32: 767-775.

[9] Bao Z, Malki MI, Forootan SS, Adamson J, Forootan FS, Chen D, Foster CS, Rudland PS and Ke Y. A novel cutaneous fatty acid-binding protein-related signaling pathway leading to malignant progression in prostate cancer cells. Genes Cancer 2013; 4: 297-314.

[10] Forootan FS, Forootan SS, Gou X, Yang J, Liu B, Chen D, Al Fayi MS, Al-Jameel W, Rudland PS, Hussain SA and Ke Y. Fatty acid activated PPARγ promotes tumorigenicity of prostate cancer cells by up regulating VEGF via PPAR responsive elements of the promoter. Oncotarget 2016; 7: 9322-39.

[11] Forootan FS, Forootan SS, Malki MI, Chen D, Li G, Lin K, Rudland PS, Foster CS and Ke Y. The expression of C-FABP and PPARgamma and their prognostic significance in prostate cancer. Int J Oncol 2014; 44: 265-275.

[12] Fujita K, Kume H, Matsuzaki K, Kawashima A, Ujike T, Nagahara A, Uemura M, Miyagawa Y, Tomonaga T and Nonomura N. Proteomic analysis of urinary extracellular vesicles from high Gleason score prostate cancer. Sci Rep 2017; 7: 42961.

[13] Kawaguchi K, Kinameri A, Suzuki S, Senga S, Ke Y and Fujii H. The cancer-promoting gene fatty acid-binding protein 5 (FABP5) is epigenetically regulated during human prostate carcinogenesis. Biochem J 2016; 473: 449-461.

[14] Naeem AA, Abdulsamad SA, Rudland PS, Malki MI and Ke Y. Fatty acid-binding protein 5 (FABP5)-related signal transduction pathway in castration-resistant prostate cancer cells: a potential therapeutic target. Precis Clin Med 2019; 2: 192-196.

[15] Berger WT, Ralph BP, Kaczocha M, Sun J, Balius TE, Rizzo RC, Haj-Dahmane S, Ojima I and Deutsch DG. Targeting fatty acid binding protein (FABP) anandamide transporters - a novel strategy for development of anti-inflammatory and anti-nociceptive drugs. PLoS One 2012; 7: e50968.

[16] Al-Jameel W, Gou X, Forootan SS, Al Fayi MS, Rudland PS, Forootan FS, Zhang J, Cornford PA, Hussain SA and Ke Y. Inhibitor SBFI26 suppresses the malignant progression of castration-resistant PC3-M cells by competitively binding to oncogenic FABP5. Oncotarget 2017; 8: 31041-31056.

[17] Al-Jameel W, Gou X, Jin X, Zhang J, Wei Q, Ai J, Li H, Al-Bayati A, Platt-Higgins A, Pettitt A, Rudland PS and Ke Y. Inactivated FABP5 suppresses malignant progression of prostate cancer cells by inhibiting the activation of nuclear fatty acid receptor PPARgamma. Genes Cancer 2019; 10: 80-96.
[18] Naeem AA, Abdulsamad SA, Zeng H, He G, Jin X, Zhang J, Alenezi BT, Ma H, Rudland PS and Ke Y. FABP5 can substitute for androgen receptor in malignant progression of prostate cancer cells. Int J Oncol 2024; 64: 18.
[19] Zhang J, He G, Jin X, Alenezi BT, Naeem AA, Abdulsamad SA and Ke Y. Molecular mechanisms on how FABP5 inhibitors promote apoptosis-induction sensitivity of prostate cancer cells. Cell Biol Int 2023; 47: 929-942.
[20] Galletti G, Leach BI, Lam L and Tagawa ST. Mechanisms of resistance to systemic therapy in metastatic castration-resistant prostate cancer. Cancer Treat Rev 2017; 57: 16-27.
[21] Tannock IF, de Wit R, Berry WR, Horti J, Pluzanska A, Chi KN, Oudard S, Theodore C, James ND, Turesson I, Rosenthal MA and Eisenberger MA; TAX 327 Investigators. Docetaxel plus prednisone or mitoxantrone plus prednisone for advanced prostate cancer. N Engl J Med 2004; 351: 1502-1512.
[22] Zhu ML, Horbinski CM, Garzotto M, Qian DZ, Beer TM and Kyprianou N. Tubulin-targeting chemotherapy impairs androgen receptor activity in prostate cancer. Cancer Res 2010; 70: 7992-8002.
[23] Guo XL, Lin GJ, Zhao H, Gao Y, Qian LP, Xu SR, Fu LN, Xu Q and Wang JJ. Inhibitory effects of docetaxel on expression of VEGF, bFGF and MMPs of LS174T cell. World J Gastroenterol 2003; 9: 1995-1998.
[24] Wang Q and Liu X. The dual functions of alpha-tubulin acetylation in cellular apoptosis and autophage induced by tanespimycin in lung cancer cells. Cancer Cell Int 2020; 20: 369.
[25] Cao W, Shiverick KT, Namiki K, Sakai Y, Porvasnik S, Urbanek C and Rosser CJ. Docetaxel and bortezomib downregulate Bcl-2 and sensitize PC-3-Bcl-2 expressing prostate cancer cells to irradiation. World J Urol 2008; 26: 509-516.
[26] Higano CS, Beer TM, Taplin ME, Efstathiou E, Hirmand M, Forer D and Scher HI. Long-term safety and antitumor activity in the phase 1-2 study of enzalutamide in pre- and post-docetaxel castration-resistant prostate cancer. Eur Urol 2015; 68: 795-801.
[27] Yu JX, Liu X and Xu B. Docetaxel induces apoptosis and influences the expression of P-gp, BCL-2 and BAX protein in HL-60/ADR cells. Zhongguo Shi Yan Xue Ye Xue Za Zhi 2010; 18: 311-316.
[28] Tran C, Ouk S, Clegg NJ, Chen Y, Watson PA, Arora V, Wongvipat J, Smith-Jones PM, Yoo D, Kwon A, Wasielewska T, Welsbie D, Chen CD, Higano CS, Beer TM, Hung DT, Scher HI, Jung ME and Sawyers CL. Development of a second-generation antiandrogen for treatment of advanced prostate cancer. Science 2009; 324: 787-790.
[29] Kim W and Ryan CJ. Androgen receptor directed therapies in castration-resistant metastatic prostate cancer. Curr Treat Options Oncol 2012; 13: 189-200.
[30] Mostaghel EA, Marck BT, Plymate SR, Vessella RL, Balk S, Matsumoto AM, Nelson PS and Montgomery RB. Resistance to CYP17A1 inhibition with abiraterone in castration-resistant prostate cancer: induction of steroidogenesis and androgen receptor splice variants. Clin Cancer Res 2011; 17: 5913-5925.
[31] Dehm SM, Schmidt LJ, Heemers HV, Vessella RL and Tindall DJ. Splicing of a novel androgen receptor exon generates a constitutively active androgen receptor that mediates prostate cancer therapy resistance. Cancer Res 2008; 68: 5469-5477.
[32] Hu R, Dunn TA, Wei S, Isharwal S, Veltri RW, Humphreys E, Han M, Partin AW, Vessella RL, Isaacs WB, Bova GS and Luo J. Ligand-independent androgen receptor variants derived from splicing of cryptic exons signify hormone-refractory prostate cancer. Cancer Res 2009; 69: 16-22.
[33] Miyamoto H, Messing EM and Chang C. Androgen deprivation therapy for prostate cancer: current status and future prospects. Prostate 2004; 61: 332-353.
[34] Guo Z, Yang X, Sun F, Jiang R, Linn DE, Chen H, Chen H, Kong X, Melamed J, Tepper CG, Kung HJ, Brodie AM, Edwards J and Qiu Y. A novel androgen receptor splice variant is up-regulated during prostate cancer progression and promotes androgen depletion-resistant growth. Cancer Res 2009; 69: 2305-2313.
[35] Hu R, Isaacs WB and Luo J. A snapshot of the expression signature of androgen receptor splicing variants and their distinctive transcriptional activities. Prostate 2011; 71: 1656-1667.
[36] Li Y, Alsagabi M, Fan D, Bova GS, Tewfik AH and Dehm SM. Intragenic rearrangement and altered RNA splicing of the androgen receptor in a cell-based model of prostate cancer progression. Cancer Res 2011; 71: 2108-2117.
[37] Li Y, Hwang TH, Oseth LA, Hauge A, Vessella RL, Schmechel SC, Hirsch B, Beckman KB, Silverstein KA and Dehm SM. AR intragenic deletions linked to androgen receptor splice variant expression and activity in models of prostate cancer progression. Oncogene 2012; 31: 4759-4767.

[38] Antonarakis ES, Lu C, Wang H, Luber B, Nakazawa M, Roeser JC, Chen Y, Mohammad TA, Chen Y, Fedor HL, Lotan TL, Zheng Q, De Marzo AM, Isaacs JT, Isaacs WB, Nadal R, Paller CJ, Denmeade SR, Carducci MA, Eisenberger MA and Luo J. AR-V7 and resistance to enzalutamide and abiraterone in prostate cancer. N Engl J Med 2014; 371: 1028-1038.

[39] Harris WP, Mostaghel EA, Nelson PS and Montgomery B. Androgen deprivation therapy: progress in understanding mechanisms of resistance and optimizing androgen depletion. Nat Clin Pract Urol 2009; 6: 76-85.

[40] Baker J, Ajani J, Scotte F, Winther D, Martin M, Aapro MS and von Minckwitz G. Docetaxel-related side effects and their management. Eur J Oncol Nurs 2009; 13: 49-59.

[41] Cella D, Peterman A, Hudgens S, Webster K and Socinski MA. Measuring the side effects of taxane therapy in oncology: the functional assesment of cancer therapy-taxane (FACT-taxane). Cancer 2003; 98: 822-831.

[42] Merseburger AS, Haas GP and von Klot CA. An update on enzalutamide in the treatment of prostate cancer. Ther Adv Urol 2015; 7: 9-21.

[43] Naeem AA, Abdulsamad SA, Al-Bayati A, Zhang J, Malki MI, Ma H and Ke Y. Prostate cell lines. J Oncol Med 2022; 5: 534-538.

[44] Mitchell S, Abel P, Ware M, Stamp G and Lalani E. Phenotypic and genotypic characterization of commonly used human prostatic cell lines. BJU Int 2000; 85: 932-944.

[45] Chou TC. Drug combination studies and their synergy quantification using the Chou-Talalay method. Cancer Res 2010; 70: 440-446.

[46] Ross RW, Xie W, Regan MM, Pomerantz M, Nakabayashi M, Daskivich TJ, Sartor O, Taplin ME, Kantoff PW and Oh WK. Efficacy of androgen deprivation therapy (ADT) in patients with advanced prostate cancer: association between Gleason score, prostate-specific antigen level, and prior ADT exposure with duration of ADT effect. Cancer 2008; 112: 1247-1253.

[47] Coutinho I, Day TK, Tilley WD and Selth LA. Androgen receptor signaling in castration-resistant prostate cancer: a lesson in persistence. Endocr Relat Cancer 2016; 23: T179-T197.

[48] Forootan SS, Hussain S, Aachi V, Foster CS and Ke Y. Molecular mechanisms involved in the transition of prostate cancer cells from androgen dependant to castration resistant state. J Androl Gynaecol 2014; 2: 1-9.

[49] Zobniw CM, Causebrook A and Fong MK. Clinical use of abiraterone in the treatment of metastatic castration-resistant prostate cancer. Res Rep Urol 2014; 6: 97-105.

[50] Karantanos T, Corn PG and Thompson TC. Prostate cancer progression after androgen deprivation therapy: mechanisms of castrate resistance and novel therapeutic approaches. Oncogene 2013; 32: 5501-5511.

[51] Katzenwadel A and Wolf P. Androgen deprivation of prostate cancer: leading to a therapeutic dead end. Cancer Lett 2015; 367: 12-17.

[52] Wang K, Ruan H, Xu T, Liu L, Liu D, Yang H, Zhang X and Chen K. Recent advances on the progressive mechanism and therapy in castration-resistant prostate cancer. Onco Targets Ther 2018; 11: 3167-3178.

[53] Khurana N, Kim H, Chandra PK, Talwar S, Sharma P, Abdel-Mageed AB, Sikka SC and Mondal D. Multimodal actions of the phytochemical sulforaphane suppress both AR and AR-V7 in 22Rv1 cells: advocating a potent pharmaceutical combination against castration-resistant prostate cancer. Oncol Rep 2017; 38: 2774-2786.

[54] Zheng Z, Li J, Liu Y, Shi Z, Xuan Z, Yang K, Xu C, Bai Y, Fu M, Xiao Q, Sun H and Shao C. The crucial role of AR-V7 in enzalutamide-resistance of castration-resistant prostate cancer. Cancers (Basel) 2022; 14: 4877.

[55] Zhu Y, Dalrymple SL, Coleman I, Zheng SL, Xu J, Hooper JE, Antonarakis ES, De Marzo AM, Meeker AK, Nelson PS, Isaacs WB, Denmeade SR, Luo J, Brennen WN and Isaacs JT. Role of androgen receptor splice variant-7 (AR-V7) in prostate cancer resistance to 2nd-generation androgen receptor signaling inhibitors. Oncogene 2020; 39: 6935-6949.